Investigation of Effects of Abrasive Blasting on Fusion Welded Joints

A Dissertation submitted
in partial fulfillment of the requirements
for the degree of

Master of Engineering

in

Production Engineering

by

Sangam Garg

(801382024)

Under the Supervision of

Dr. V.K. Singla
Associate Professor

Dr. Vivek Jain
Assistant professor

MECHANICAL ENGINEERING DEPARTMENT

THAPAR UNIVERSITY, PATIALA

July, 2015

CERTIFICATE

I hereby declare that the thesis entitled "**Investigation of Effects of Abrasive Blasting on Fusion Welded Joints**" is an authentic record of my work carried out as requirements for the award of the degree of **Master of Engineering** in **Production Engineering** at **Thapar University, Patiala** under the supervision of **Dr. V.K. Singla**, Associate Professor, Mechanical Engineering Department and **Dr. Vivek Jain**, Assistant Professor, Mechanical Engineering Department, Thapar University, Patiala during July, 2013 to July, 2015. No part of the matter embodied in this report has been submitted to any other University or Institute for the award of any degree.

Date: 15-7-15

Sangam Garg
801382024

It is certified that the above statement made by the student is correct to the best of my/our knowledge and belief.

Dr. V.K. Singla
Associate Professor
Mechanical Engg. Department
Thapar University, Patiala - 147004

13/7/15

Dr. Vivek Jain
Assistant Professor
Mechanical Engg. Department
Thapar University, Patiala - 147004

Countersigned by

Dr. S.K. Mohapatra
Head, Mechanical Engineering Department
Thapar University, Patiala – 147004

Professor S.S. Bhatia
Dean of Academic Affairs
Thapar University, Patiala – 147004

Acknowledgement

It gives me a great sense of pleasure to present the report of the thesis work undertaken during ME second year. I owe special debt of gratitude to **Dr. V.K. Singla, Associate Professor, Department of Mechanical Engineering** and **Dr. Vivek Jain**, **Assistant Professor, Department of Mechanical Engineering** for his constant support and guidance throughout the course of our work. His sincerity, thoroughness and perseverance have been a constant source of inspiration for us. It is only his cognizant efforts that our endeavors have seen light of the day.

I also take the opportunity to acknowledge the contribution of **Dr. S.K. Mohapatra, Senior Professor and Head, Department of Mechanical Engineering** for his full support and assistance.

I also do not like to miss the opportunity to acknowledge the contribution of all faculty members of the department for their kind assistance and cooperation. Last but not the least, I acknowledge my friends for their contribution in this work.

Sangam Garg

(801382024)

Abstract

Fusion welding is a metal joining process used largely in industries. In fusion welding, high temperature melts the metal and joins the components. There are three types of fusion welding processes- Gas, Arc and High-energy beam welding. The present research focuses on Arc type- submerged arc welding (SAW), manual metal arc (MMA), tungsten inert gas (TIG), metal inert gas (MIG). Although fusion welding is widely used, there are many concerns about the weld quality. The problems faced are porosity, undercut, incomplete joint penetration, stresses etc. These defects affects the tensile strength, hardness, fatigue life of the joint. The welded parts also experiences melting and solidification process, dissolution of gases, distortion which leads to change in microstructural behavior and also changing the composition of the parts. To improve and enhance the properties abrasive blasting can be done. This study will attempt to provide the comparison of effects of abrasive blasting on fusion welded joints of low carbon and medium carbon steel. Input parameters are 4 different arc welding processes and 4 different shot blasting time periods. The output parameters will be Surface hardness, Tensile strength, Microstructure and fractography.

Keywords: MMA, MIG, TIG, SAW, VHN, Abrasive Blasting

Table of Contents

List of Figures

List of Tables

Acronyms

FZ	≡	Fusion zone
HAZ	≡	Heat affected zone
BM	≡	Base Metal
MMA	≡	Manual metal arc
MIG	≡	Metal inert gas
TIG	≡	Tungsten inert gas
SAW	≡	Submerged arc welding
A.C.	≡	Alternating Current
D.C.	≡	Direct Current
AAS	≡	Atomic absorption spectroscopy
PJL	≡	Plate joint line
VHN	≡	Vickers hardness number
LOP	≡	Lack of penetration

CHAPTER 1

Introduction

1.1 Introduction

Manufacturing technology can be classified into four main processes: Casting, machining, joining or welding and forming. The selection of the process depends upon various factors like number of units to be produced, complexity of the shape, desired material properties and size of the product. Casting and forming are zero process as in these no material is added or removed, only shifting of metal is done with the help of pressure and heat. Machining is a negative process as in machining material is removed in the form of small chips. Joining or welding is a positive process as in this material is added in the form of filler wire or assembling different products in a permanent or temporary joint. Welding or joining is a frequent process used in industries and it is of three types: mechanical joints (which is done with the help of nuts, bolts and rivets), adhesive joints (usage of epoxy resins etc.) and welding. The selection of joining is done on the requirement of joints whether temporary or permanent, amount of load to be carried, environment in which joint is used, reliability of the joint and compatibility of metals to be joined. Welding is a process of joining two metals whether similar or dissimilar with or without application of pressure, with or without heat and with or without use of filler wire so as to produce a strong joint with desirable mechanical properties.

Welding can be classified into various types: Gas welding, solid state welding, arc welding, resistance welding and thermo-chemical welding process. Though there are 94 different types of welding processes recognised by the AWS (American welding society) that uses different types of energy sources for welding, Arc welding is still the most popular welding process. Arc processes can be further classified into manual metal arc welding (MMA), submerged arc welding (SAW), tungsten inert gas welding (TIG), flux coated arc welding, plasma arc welding and metal inert gas welding (MIG).

Carbon steel is a type of alloying element which mainly consists of Iron and Carbon. Several other elements can be also added in various percentages upon the desired properties. The elements added

are Manganese, 1.65% max., 0.6 % max. Silicon and 0.6 % max copper. Other elements can also be added but in small quantities. Carbon steel can be further classified according to percentage of the carbon in the alloy: low carbon steel (0.05%-0.22% C), medium carbon steel (0.24% to 0.5% C), high carbon steel (0.51% to 0.95% C) and very high carbon steel (0.98% to 2% C). Lower carbon steel is soft in nature, medium carbon steel has better ductility and hardness, high carbon steel and very high carbon steel has very high hardness but low ductility. In this present work different types of arc welding are done on low carbon steel and medium carbon steel.

1.2Welding

Welding is a permanent type of joint which affects the metallurgical properties of the material. Normally post-heat treatment is done to improve the properties of the welded joint. Welding usually requires heat or pressure to join two different components [Ghosh and Mallik, 1985]. There is also processes similar to welding which uses low melting point filler metal to join metals having higher melting point. These allied processes are soldering and brazing. Welding process equipment can also be used for cutting of the metals. Welding can be manual, semi-automatic and automatic. Normally manual welding was done but with the need of weld requirement in hazardous environment or getting higher productivity automatic welding processes are being developed.

1.2.1 Classification of Welding

Welding can be classified by various categories: whether we use filler wire or not, what type of energy source is being used (Chemical, Mechanical, Electrical and Radiation), whether we use heat or pressure for welding. Fig. 1.1 shows one type of classification.

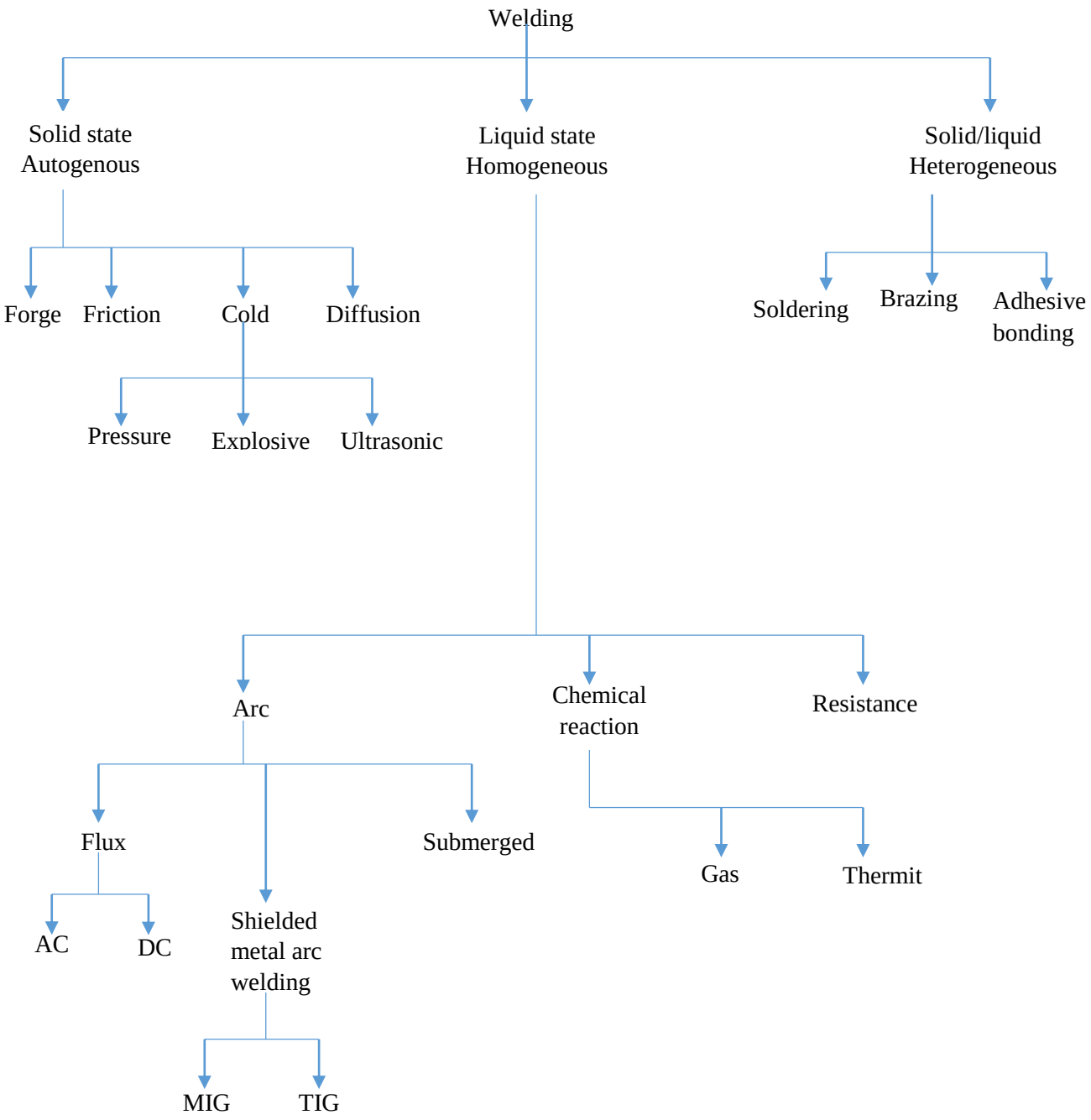

Figure 1.1: Classification of welding processes

1.3 Manual Metal Arc Welding (MMA)

It is a most common arc welding process which uses consumable coated electrode. As the coating on the electrode burns during welding, it disintegrates and forms a protective shield around the weld area protecting it from oxidation and absorption of the nitrogen. The electrode after melting produces slag which covers the molten filler metal and protects it till metal solidifies. Slag can be easily chipped away with chipping hammer after solidification. Fig. 1.2 shows the MMA welding.

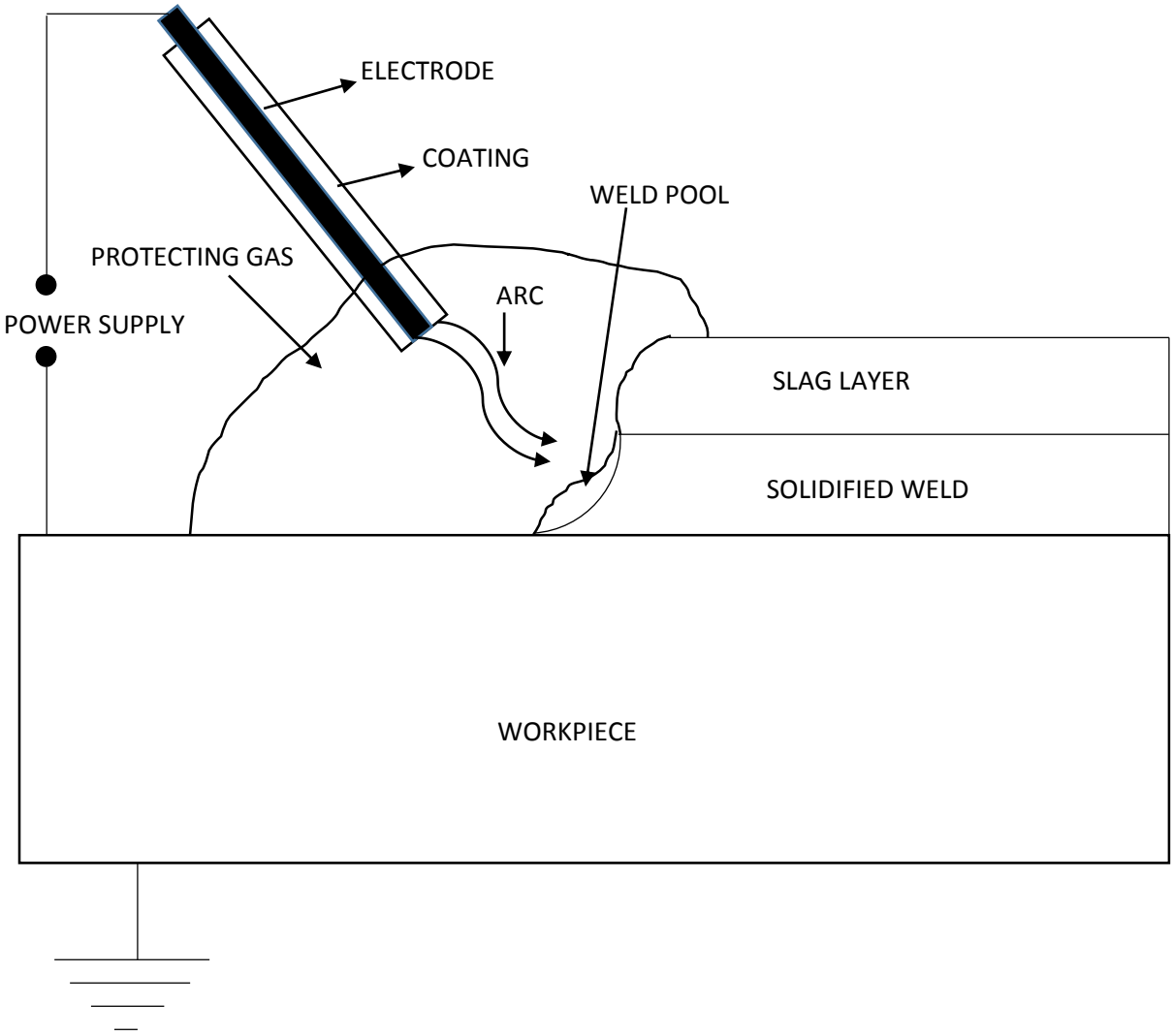

Figure 1.2: A schematic of MMA welding process

1.4 Metal Inert Gas Welding (MIG)

MIG welding is a semi-automatic or automatic arc welding process in which arc is generated between electrode and work piece due to continuous feed of wire from the spool. In general, constant voltage source with direct current (DC) is generally used but constant current with alternating current power source can also be used. It works on the principle of arc generation in which ions are transferred from electrode to work piece. In this work piece is connected to one terminal and electrode is connected to another terminal. Fig. 1.3 shows the MIG welding process.

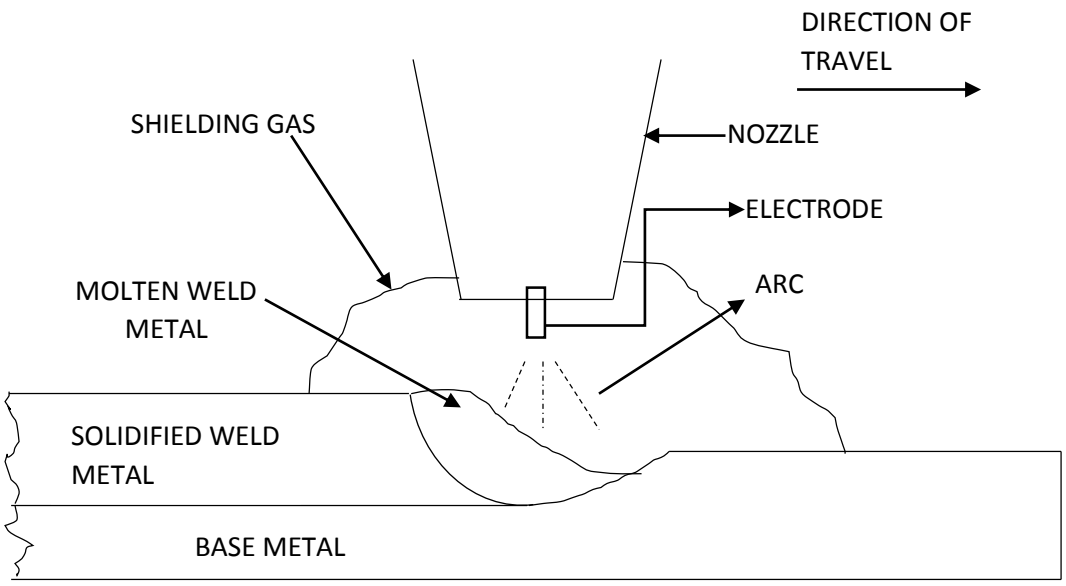

Figure 1.3: A schematic of MIG welding process

1.4.1 Advantages of MIG Welding

MIG welding is mostly used in industries because it can weld a variety of materials. Some advantages of MIG welding which are discussed below

- MIG welding is faster as compare to other welding because wire is fed continuously.
- It can weld both thin and thick materials.
- It can be automatic or semi-automatic according to the need. So it is very flexible.
- It does not require any flux to remove.

- It gives clean, smooth, stable and high quality weld.
- Due to high travel speed, it generates less distortion.
- It generates fewer amounts of fumes.
- It can weld in all positions.
- It can weld both ferrous and non-ferrous metals.

1.4.2 Disadvantages of MIG Welding

There are some disadvantages of MIG welding which are discussed below.

- The equipments of MIG welding are complex and they are difficult to understand.
- It generates unstable arc. Due to this it produces burn back.
- It is not suitable for outdoor applications because air can disturb its shielding gas envelope.
- In this welding there is a problem of irregular wire feed.
- There is a possibility of porosity, incomplete fusion and crack in MIG welding.

1.4.3 Applications of MIG Welding

- It can weld a variety of materials like both low and high alloy, ferrous and non-ferrous material, aluminum, titanium and other materials alloys.
- It can be used for automotive repair and pipe joints.
- It is used in industries for making large products like pressure vessel, ship parts and other automobile parts.
- It is used in refrigeration industry.

1.5 Tungsten Inert Gas Welding (TIG)

Tungsten inert gas welding (TIG) uses non consumable tungsten electrode to weld the metal. It uses shielding gases like Argon, Helium or mixture of both. A filler wire maybe supplied during the weld according to need. The shielding gases forms a blanket around the weld so as to protect it from atmospheric gases and other contaminants. Fig. 1.4 shows the TIG Welding process.

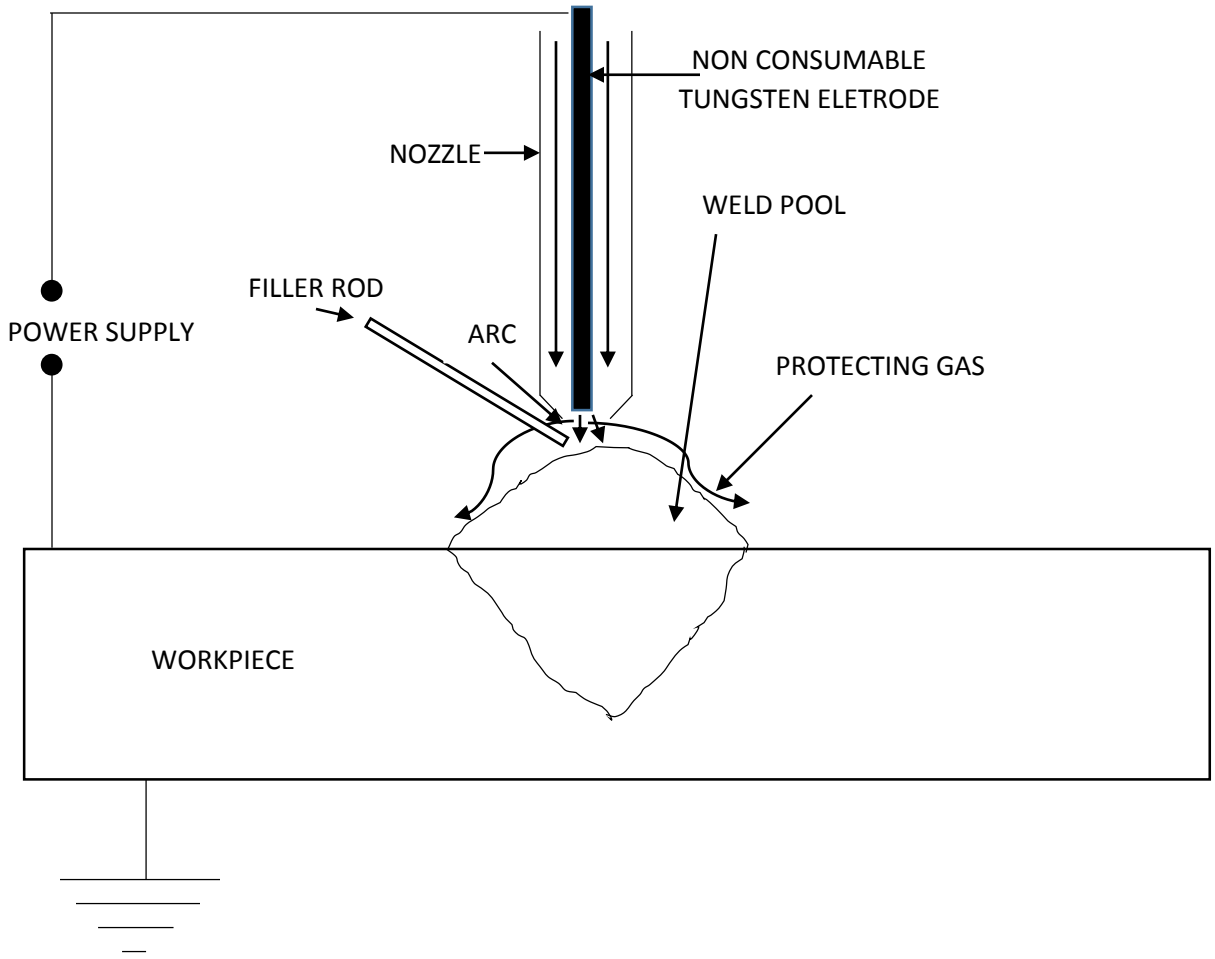

Figure 1.4: A schematic of TIG welding process

1.5.1 Advantages of TIG Welding

- It can be used to weld unlike metals
- Heat affected zone is very low.
- It can be used to weld reactive metals like Aluminium, Magnesium etc.
- No slag is produced
- Low levels of smoke is produced
- Less distortion

1.5.2 Disadvantages of TIG Welding

- It is a slower process than consumable electrode arc welding processes
- Skilful worker is required
- Radiations from TIG welding are higher as compared to other arc welding processes.
- Cost is high due to expenses of gases and slow speed

1.5.3 Applications of TIG Welding

- Nuclear reactors
- Offshore industry
- Chemical industry
- Petrochemical industry
- Food industry

1.6 Submerged Arc Welding (SAW)

It is an automatic process developed for producing butt welds in thicker steel plates. In SAW, a blanket of fusible, granular material is used for shielding the metal during the welding. The penetration is deep in this process and weld deposition rate is high. The electrode wire is automatically supplied by machine units also controlling its feed. The arc takes place beneath the flux and hence this is known as submerged arc welding. Fig. 1.5 shows a schematic of SAW process.

1.6.1 Advantages of SAW Welding

- Weld spatter is eliminated
- 100% deposition efficiency is achieved
- High welding speeds are possible
- Wire electrodes are inexpensive
- High operating factors in mechanized applications

1.6.2 Disadvantages of SAW Welding

- It cannot be used for plates less than 5 mm thick
- Requires relatively troublesome flux handling systems
- Requires inter-pass and post weld slag removal
- Limited to ferrous and some nickel-based alloys

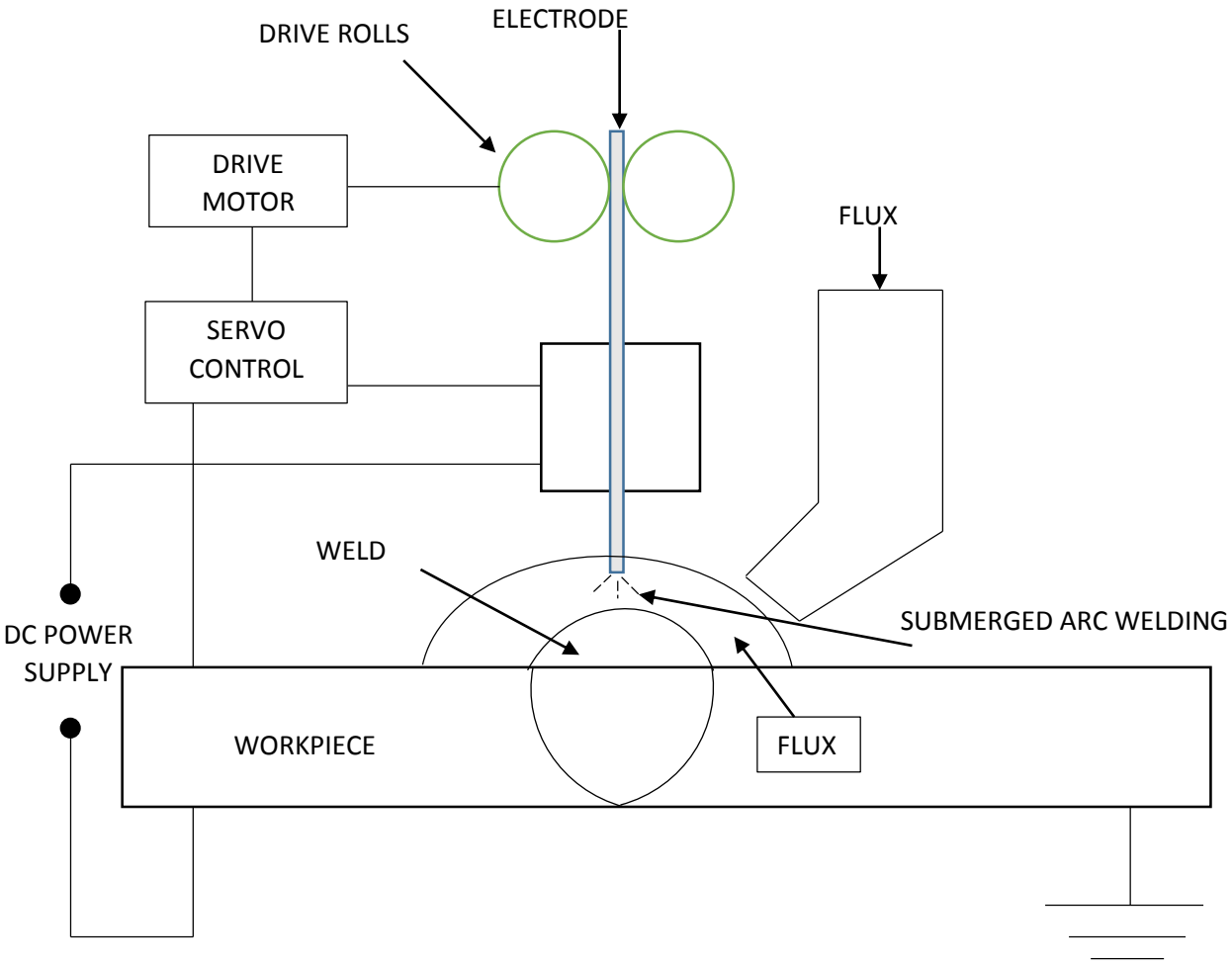

Figure 1.5: A schematic of SAW welding process

1.7 Abrasive Blasting

Abrasive blasting is the process of forceful direction of abrasives on the material for cleaning, roughening, finishing and machining. A centrifugal wheel or pressurised air is used to propel the abrasives. Abrasives are of various types like sand, slag, steel shots, glass beads etc. Several variants of abrasive blasting are bead blasting, sand blasting, shot blasting, shot peening, hydro blasting and wet blasting. Modern cemetery monuments uses abrasive blasting for lettering and engraving. Micro blasting of cutting tips and tools is a very effective and reliable method of advancing the life of tools under the action of turning, milling, drilling, punching and cutting. Shot peening is a cold working process which uses spherical steel shots for bombardment [Kim, 2013]. Due to bombarding of steel balls compressive residual stresses are produced. To have a permanent effect, material must yield in tension which will lead to elastic stretching of the upper surface and local plastic deformation will occur, thus yielding compressive stresses in the depth [Meo and Vignjevic, 2003]. The greater the magnitude and depth of residual stresses, greater increase in the mechanical properties of the material [Habibi et al., 2012]. Now as abrasive blasting generates compressive residual stresses, so there will be no crack formation as cracks doesn't generate in compressive residual stresses. Shot blasting helps in roughening of the surface which helps in adhesion bond.

Welding has many types of defects: Voids, gas inclusions, porosity, tensile stresses which reduces the mechanical properties of the joints. To overcome this abrasive blasting is a common process used in industries. Abrasive blasting is a process of blasting abrasives on the material using high pressure to smoothen a rough surface, roughen a smooth surface, material removal, changing properties and removing the surface contaminants. Abrasive blasting has various variants like: shot peening, sand blasting, shot blasting and bead blasting. Abrasive blasting helps in producing residual compressive stresses to counter the tension stresses produced during welding, it also helps in surface hardening and removing the surface irregularities.

CHAPTER 2

Literature Review

2.1 Introduction

Fusion welding is a conventional welding process that can be defined as a process used to join two pieces of metal by application of heat. The two parts to be joined are cleaned, then the cleaned surfaces are placed together, heated, until they melt and solidify on cooling. A pool of molten metal forms and connects the components, and a filler rod may be used to add metal to the joint. Placing a fusion weld in a structure may lead to a variety of discontinuities, including porosity, incomplete joint penetration, undercut conditions, and cracking (which is often caused by stress concentrations near discontinuities in the weld and base metal) [Lah et al., 2010]. Thus, this study attempts to provide a solution by applying abrasive blasting treatment. The process involves bombarding of surface of weld joints by spherical media called shot, which strikes the material like tiny hammers. This introduces beneficial compressive residual stresses and thus build up tension is relieved. The other benefits of abrasive blasting are uniform cleaning, surface hardening but it also increases the surface roughness of the workpiece.

2.2 Literature Review

Berezhnyts'ka et al. (2000) investigated the effects of pneumatic shot blasting of steel balls with 1 mm dia. with pressure 0.4 MPa for 60 sec on 08Kp, 08GSYuT, 07GSYuFT steel. The shot blasting was done on both sheets and arc welded joints of thickness 1.2 mm. The sheet and arc welded joints was forge rolled for further testing. The fatigue test was conducted on sheets and welded joints in air and in 3% NaCl solution. The fatigue and corrosion fatigue resistance of low alloy steels increases by 29%. The increase in values of 08Kp was far greater than of 08GSYuT steel. For increasing the cyclic and low-cyclic durability of steels, shot blasting proves to be an efficient process. The increase in cyclic durability was less in case of corrosion environment as compared to the air.

Aparicio et al. (2003) investigated the effect of shot blasting on commercial pure titanium. 6 mm disc of titanium was taken for experimental purpose. Topographical features and electrochemical behavior was tested. Shot blasting was done through different medias: Al2: Al_2O_3 of 200 µm, Al6: Al_2O_3 of 600 µm, Al9: Al_2O_3 of 900 µm, Si2: SiC of 200 µm, Si6: SiC of 600 µm, Si9: SiC of 900 µm. Surface roughness of titanium increases due to shot blasting which was colonized by bone and helpful in implant fixation. Chemical composition of titanium also changes due to balls adhered in the surface. The value of surface roughness changes according to size of balls, larger the size of balls higher the value of surface roughness. Coverage rate was found higher in the case of large size balls. SiC has greater effect on the properties than Al_2O_3.

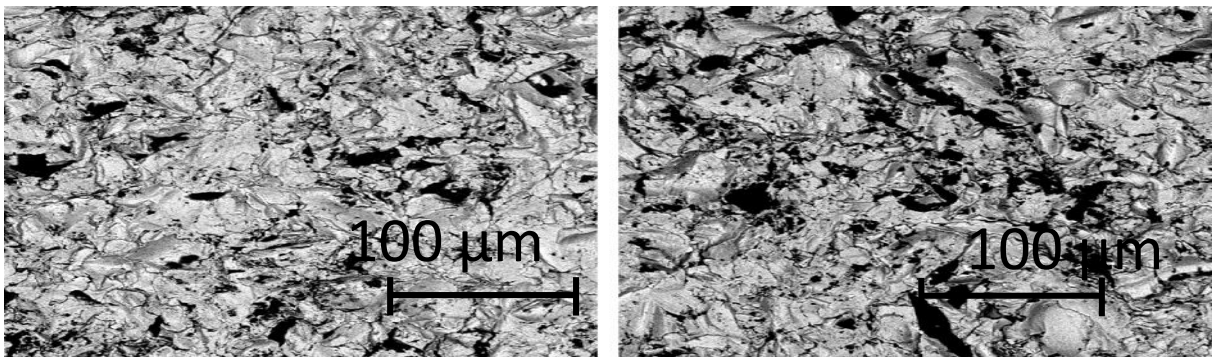

Fig. 2.1: Comparing example of BS-SEM images for Si6 (left) and Al6 (right), where the dark areas correspond to attached particles

Meo et al. (2003) described finite element analysis of residual stress induced by shot peening process. It presents the modeling and simulation of the residual stress field resulting from the shot peening process. The ball was made of hard steel while the material work-piece was made of Aluminum 2024-T6. The diameter of the ball to use depends on the material and thickness of component to be shot-peened, but in this analysis the diameter of the ball used is 3 mm. The impacting speed is 36 m/s. The results achieved show that the use of shot peening process would improve significantly the structural performance of welded joints. This was due to the fact that imposing a compressive longitudinal residual stress generated by the forming process would lower or annul the tensile residual stress field generated by the welding process.

Hasegawa et al. (2004) studied the effect of shot blasting on SM 490A rolled steel plates. 6 mm thick plate of SM 490A was welded using MAG closed square butt welding in two phases, 1st at face and 2nd as back. Welding parameters taken were 270A as welding current, 27 V as welding voltage and 470 mm/min as welding speed. Mixture of argon and carbon dioxide was used as shielding gas with gas flow rate of 16 l/min. Shot peening was done with tungsten carbide (150 µm and 100 µm) and steel of 177 µm impacted at an angle of 45°. Different air pressures used for tungsten carbide of 150 µm were 0.12, 0.2, 0.3, 0.4 and 0.5 MPa, for tungsten carbide of 100 µm were 0.2, 0.3, 0.4 and 0.5 MPa and for steel of 177 µm were 0.2 and 0.5 MPa. There was fatigue life increase even at 0.2 MPa. Increase in fatigue life was due to hardness rise which contributes to increase in compressive residual stress.

Kennedy et al. (2005) described micro shot blasting of machine tools for improving surface finish and reducing cutting forces in manufacturing. Tool made up of Tungsten Carbide and high speed steels were subjected to micro blasting using shot media ceramic bead of 40 µm with impact angle of 90º. Testing of treated and untreated cutting tips and tool was conducted on HSSs for turning and milling as well as coated and uncoated carbide inserts. These tools performances were tested on lathe and milling machines. Tool surfaces showed increase in toughness, improving hardness and surface finish. Dynamometer were used to measure cutting forces for both treated and untreated processes and it showed that treated tools can be used for much higher rpm. Thus increasing operating life of these tools.

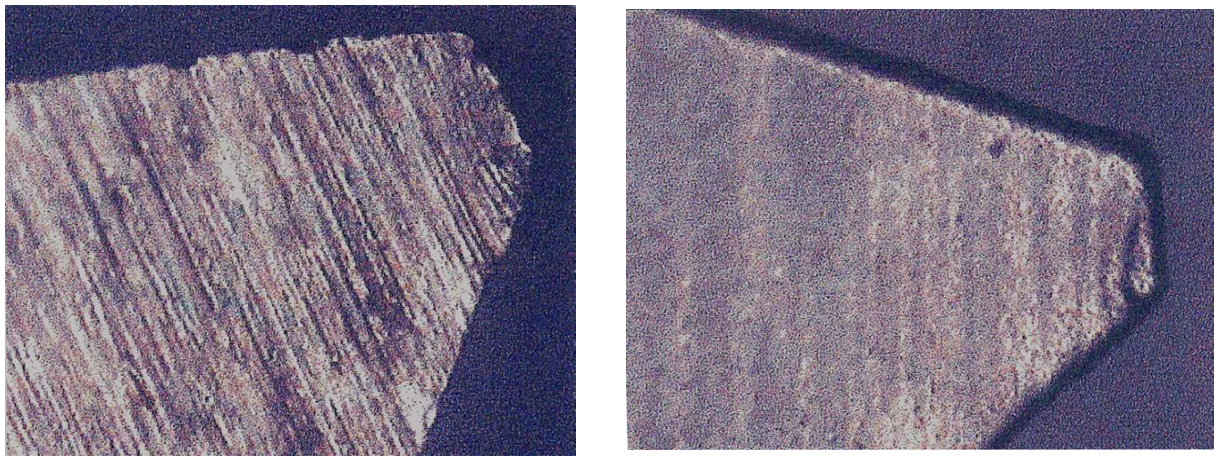

Fig. 2.2: High speed steel tip prior and after treatment

Sidhom et al. (2005) studied the effect of shot peening on MIG welded T-joints 5083 H11 Al alloy. Al alloy welding wire of 5183 was used as weld material. Four point bending test was done to find out the fatigue value. Shot peening was done using steel shots of specification MI-330R with coverage rate of 125%, strike angle of 90° and Almen intensity of 16-20 A. Residual stresses was checked at weld toe before and after shot peening. Fatigue test was done at two different stress ratios of 0.1 and 0.5. The enhancement of fatigue strength was higher in the case of stress ratio of 0.5 than 0.1. Increment in fatigue life was 135% and 59% in case of stress ratio of 0.5 and 0.1 respectively.

Zivkoviv et al. (2005) studied the effect of shot peening on TIG welded Al alloy 5803. A single V-shaped butt welding was done taking angle of 90°. TIG welding was done on 6.5 mm thick plate taking root of 3mm with welding parameters of current 190 A and voltage 20 V. Shot peening was done with the help of S390 at angle of 90° and temperature value of 25° C. Shot peening was done at three different intensities that were 0.5, 0.7 and 0.9 Almen intensity. The value of fatigue life at 10^5 cycles is 75% greater than 10^6 cycles. The increase in fatigue life of shot peened samples were 59% in 10^5 cycles and 93% in 10^6 cycles with Almen intensity of 0.9. With increase in Almen intensity the effect of shot peening also increases i.e. increase in fatigue life.

Naidu et al. (2005) investigated the effect of shot blasting on Al-Mg-Si alloy AA6061. 8.3 mm thick plate of length 65 mm and 10 mm width was chosen. For shot blasting spherical balls of aluminum oxide of size 120 µm with a stand-off distance 100 mm, 100 s blasting time, 100% coverage rate and pressure of 0.4 MPa was chosen. The alloy was solution treated at 540°C for 1 h and water quenched to room temperature and then aged at 160° C for 12 h. The alloy after above treatment was known as T6 condition. Fatigue life reduction factor of 4 and 4.6 was found in T6 condition and shot blasted condition respectively at maximum cyclic stress of 169 MPa was found due to fretting. At higher value of max cyclic stress effect was diminished. Shot blasting increased the fatigue life factor by and in plane fatigue and fretting fatigue respectively at 169 MPa maximum cyclic stress. At higher value of maximum cyclic stress the effect of shot blasting on plane fatigue and fretting fatigue was less significant. At fretting interface value of coefficient of friction increases till 3000 cycles then remain constant. At 169 MPa maximum cyclic stress, the shot blasting has better effect on coefficient of friction than T6 as when compared at 265 MPa maximum cyclic stress.

Lobanov et al. (2006) described enhancement of the service life of welded metal structures by high- frequency mechanical peening. High-frequency mechanical peening of welded joints of structural steels of different strength grades and aluminum alloys were done. High-frequency mechanical peening was a highly productive and economical method of enhancing the service life of welded metal structures of steels of different strength and aluminum alloys at the stages of their manufacture and operation. The efficiency of HFMP of welded joints increases with the strength of the metal and working-stress concentration, depending on the weld shape, as well as with decrease in the loading cycle asymmetry.

Hui et al. (2007) described effects of shot peening on thermal cycling lifetime of TBCs prepared by EB-PVD with ZrO_2-8 wt.% Y_2O_3 (8YSZ) as top coat and CoCrAlY as bond coat on disk shaped Ni based super alloy. The Ni based super alloy specimens was of 1.5 mm thickness on which a coat of 50µm thick Co-20Cr-11Al-0.8Y was deposited. Al_2O_3 shots of 300 µm in dia. was impinged using pressure of 0.2MPa and a working distance of 280 mm. Another coating of 8YSZ of 65 µm thick was deposited. The specimen was heat-treated in air for 2 h at 973K and again for 2 h at 1273K. Thermal cycling tests were performed in air by cyclically heating the specimens at 1273K for 55 min followed by forced air cooling for 5 min. The shot peening results in increased micro-hardness and surface finish. It also gave excellent oxidation resistance due to which it gave a satisfactory thermal cycle lifetime of 1643 cycles at 1293K.

Ali et al. (2007) studied the effects of shot peening on friction stir welded joints of Al alloy 2074-T3. Microstructure and fatigue properties were tested. 13 mm thick plates of Al alloy was friction welded using rotational speed of 200 rpm in clockwise direction and feed rate of 120 mm/min. Shot peening was done with the help of S230 with coverage rate of 200% and Almen intensity of 14A. Microstructure properties were tested on as welded, un-skimmed peened samples and 3 mm skimmed peened samples. Microstructure test shows voids and cracks in as welded and unskimmed samples. But in skimmed peened samples there was no visual voids or cracks. Surface irregularities were due to inclusion of potassium and silicon oxides which was removed in skimmed samples. Due to skimming stress zone changes its position and shifts to nugget zone. The effect of shot peening was visible on both low stress cycles and high stress cycles. The change in fatigue life was due to induced residual compressive stresses in the joints.

Hasegawa et al. (2009) studied the effect of shot peening and galvanizing on steel welded joint. 6 mm thick plate of SM490A was butt welded using MAG welding with parameters as welding current 270 A, voltage 27 V and mixture of Argon and Carbon dioxide as shielding gas. Steel shots of size 600 µm was impacted using optimum angle. Then shot peened samples were pickled in nitric acid, cleaned in water for 1 min, immersed in zinc ammonium Chloride aqueous solution then dipped in Zinc for galvanizing. The fatigue limit of shot peened welded joint increase from 254 MPa to 300 MPa. The fatigue limit of shot peened base metal increases from 245 MPa to 320 MPa. After shot peening it provides a clean environment so that hot galvanizing can be done immediately. The increase in fatigue life after shot peening was due to increase in hardness, surface roughness and increase in compressive residual stress.

Kameyama et al. (2009) described effect of micro ploughing during fine particle peening process on the microstructure of metallic materials. The mechanism of microstructural changes induced by fine particle peening (FPP) treatment was analyzed. Material used for the experiments is Ti6Al4V alloy and a peening time ranging from 0.1 to 30 s. Particles plough the material aside when they collide with the surface which covers the transferred fragments, and then mixes them into the material during FPP treatment. This mixing behavior transports the transferred elements to the interior of the material which creates the lamellar microstructure containing the particle elements.

Hatamleh (2007) investigated the effect of shot peening and laser peening on friction stir welded AA 2195 joints. 12.5 mm thickness of AA 2195 was friction welded using rotation speed of 300 rpm in clockwise direction and a translation speed of 15 cm/min. Residual stresses distribution was investigated at surface and through-thickness. Weld region of 0.5 mm thickness was milled using small increments to avoid extra residual stresses. For shot peening, 0.9 mm glass beads with Almen intensity of 0.008-0.012 A and 200% coverage rate using optimum angle of 75°. Laser peening was done using laser power density of 5 GW/cm^2 for 18 ns duration. The tensile residual stresses was found to be replaced by compressive residual stresses. The residual stresses found in as welded specimens were 143 MPa which converted to -160 MPa and -179 MPa for shot peening and laser peening respectively. The depth of compressive residual stresses in case of laser peening was found to be greater than shot peening process.

Hatamleh et al. (2009a) investigated the effect of shot peening and laser peening on friction stir welded AA 7075-T7351 joints. 6.35 mm thickness of AA 7075 was friction welded using rotation speed of 350 rpm in counter-clockwise direction and a translation speed of 2.54 cm/min. Residual stresses distribution was investigated at surface and through-thickness. Weld region of 0.4 mm thickness was milled using small increments to avoid extra residual stresses. For shot peening, 0.59 mm glass beads with Almen intensity of 0.008-0.012 A and 100% coverage rate using optimum angle so that balls does not collide with rebounding balls. Laser peening was done using laser power density of 5 GW/cm^2 for 18 ns duration. The welded plates was aged from T651 condition to T 7351. Radiography and penetration test was done to check crack and voids. No visual cracks and voids was found. The fatigue strength was tested on un-peened samples, shot peened and laser peened samples and it was best in case of laser peened as compared to unpeened and shot peened samples. The tensile residual stresses was found to be replaced by compressive residual stresses. The depth of compressive residual stresses in case of laser peening was found to be greater than shot peening process.

Hatamleh et al. (2009b) investigated the effect of shot peening and laser peening on friction stir welded AA 2195 and AA 7075-T651 joints. 12.5 mm thickness of AA 2195-T8 and AA 7075-T651 was friction welded using rotation speed of 300 rpm in counter-clockwise direction and a translation speed of 15 cm/min. Residual stresses distribution was investigated at surface and through-thickness. Through thickness bulk residual stresses was measured using contour method. Weld region of 0.4 mm thickness was milled using small increments to avoid extra residual stresses. For shot peening, 0.59-0.76 mm glass beads with Almen intensity of 0.008-0.012 A and 200% coverage rate using optimum angle so that balls does not collide with rebounding balls. Laser peening was done using laser power density of 5 GW/cm^2 for 18 ns duration. Hardness profiles was measured at various distances and found to be higher in center region then decreasing till a point then again increasing. The surface residual stress was found to be higher in both AA 2195 and AA 7075 due to cold working. However deeper stresses was found in case of laser peening. In case of laser peening mid region tensile stresses was found which was necessary to compensate larger values of surface compressive stresses. Laser peening has less residual stresses near the edges.

Hatamleh et al. (2009c) investigated the effect of shot peening and laser peening on friction stir welded AA 2195 joints. 12.5 mm thickness of AA 2195 was friction welded using rotation speed of 300 rpm in clockwise direction and a translation speed of 15 cm/min. The testing was done on elevated temperature (182º C) and Cryogenic temperature (-100º C) Residual stresses distribution was investigated at surface and through-thickness. Weld region of 0.5 mm thickness was milled using small increments to avoid extra residual stresses. For shot peening, 0.9 mm glass beads with Almen intensity of 0.008-0.012 A and 200% coverage rate using optimum angle of 75°. Laser peening was done using laser power density of 5 GW/cm^2 for 18 ns duration. The tensile residual stresses was found to be replaced by compressive residual stresses. At elevated temperature, increase in yield strength in weld nugget region due to laser peening was 28% while in case of shot peening it was mere 8%. In thermos-mechanical affected zone increase in yield strength was more in the case of laser peening as compared to shot peening. In case of cryogenic temperature also resulted in tensile strength but difference between peened sample and unpeened samples was diminished. The decrease in grain size of the surfaces increases the mechanical properties of the joint.

Hatamleh et al. (2009d) investigated the effect of shot peening and laser peening on friction stir welded AA 2195 joints. 12.5 mm thickness of AA 2195 was friction welded using rotation speed of 300 rpm in clockwise direction and a translation speed of 15 cm/min. Surface roughness and friction coefficient was investigated at surface. Weld region of 0.5 mm thickness was milled using small increments to avoid extra residual stresses. For shot peening, 0.9 mm glass beads with Almen intensity of 0.008-0.012 A and 200% coverage rate using optimum angle of 75°. Laser peening was done using laser power density of 5 GW/cm^2 for 18 ns duration. Tri-bological properties was tested to find out the friction coefficient. Atomic force microscopy was done on root side to find out the surface roughness characterization. Stylus was moved in both and Y direction to find out the surface roughness at both root and crown side. Second test was done using 440 C ball slider with speed (0.5 and 3cm/s) and contact force (2 N and 10 N). Surface hardness shows softening on welded joints due to thermal cycles. Hardness was recovered through peening. Highest value of surface roughness was found in the case of shot peening as compared to un-peened and laser peened samples. Highest surface was at weld nugget due to lower hardness at that point. Atomic force microscopy reveals that high anisotropy was found in the case of un-peened and laser peened samples while shot peened samples has less anisotropy. Atomic force microscopy also reveals that

at base metal shot peened samples has large difference in surface roughness as compare to laser peened and unpeened samples but there was a minimal difference in surface roughness at other zones.

Lah et al. (2010) studied the effect of controlled shot peening on fatigue strength of ASTM A56 grade 70 carbon steel welded joint. 6.8 mm thick plate was used for MMA, MIG, and TIG welding. A Double-V butt joint shape was used to join two plates. Shot peening was done with shot of size S170 with intensity of 14-16A. Skimming of top surface of 1 mm was done to remove defects like oxide inclusion, microstructure irregularities and internal discontinuities. Hardness was tested on top and bottom surface of the welded joint and found to be higher in heat affected zone as compared to Fusion Zone. Radiography was done to check the surface irregularities and various crack zones in the weld region. Lack of penetration was found to be main reason for cracking. Fatigue test was done on as welded and shot peened samples. Increment of fatigue limit of 53%, 63 %, and 60% was found in MMA, MIG, TIG was found respectively. The best results was found in TIG welding due to high hardness, full penetration, less internal porosity and low oxygen inclusions.

Zhao et al. (2011) studied the effect of ultrasonic peening on T-shape tubular joints of 20 steel. Fatigue stress was done at three conditions- as welded, ultrasonic treatment before loading and ultrasonic treatment after loading. Ultrasonic treatment was done with speed of 1-1.5 m/min with excitation current of 2A. Ultrasonic treatment before loading was better in case of low stress ratio. But in the case of high stress ratio, ultrasonic treatment after loading was better in case of high strength steel. This was due to induced residual compressive stress which was very helpful to increase the fatigue life of the welded joints.

Sano et al. (2012) investigated the effect of laser peening without coating on friction stir welded Al alloy A6061-T6. 3 mm Al alloy plate was taken. Friction stir welding was done with rotational speed of 1400 rpm in counter-clockwise direction, translation speed of 41 mm/min and pitch angle of 3°. Laser peening was done using Nd:YAG laser. Parameters taken for laser peening were energy pulses of 60 mJ and power density of 2 GW/cm^2. Plane bending fatigue test was done on base metal, as welded and laser peened samples. Value of fatigue life in base metal increases from 90 to 120 at 10^7 cycles after laser peening. In welded material value of fatigue life increases from 90 to 120 after laser peening. Laser peening recovers the loss in hardness after welding. Surface

finish was improved. Surface finish can be optimized so as to avoid surface irregularities which initiates cracks.

Habibi et al. (2012) investigated effects of shot peening on fatigue life of six tubular X-joints made of St52 steel. Welding was done in three passes, root pass, filler pass and precision pass. Shot peening was done with the help of steel shots of size .3 mm dia. and hardness value of 45 R_c. Shot was impacted at a speed of 50 m/s and Almen intensity of 8A. Compressive residual stresses was induced in the structure thus leading to reduction in overall stress. Fatigue life was found to be increased in cyclic and low-cyclic region. For post welding treatment for off-shore structure shot peening can be recommended.

Abdullah et al. (2012) investigated the effects of ultrasonic peening treatment on SS-304 TIG welded joints. 5 mm thick plate of SS-304 was butt welded. DCEN polarity was used with 25 V and current value of 110 A. Ultrasonic peening was done with power 100 W, 20 KHz for 1 min. Titanium tool with round rod with a flat tip of 3 mm dia. was used. Fatigue, metallographic, microhardness and corrosion resistance test was done. Metallographic test shows the difference in microstructure of the peened and un-peened samples. Unpeened samples shows the crack, voids in the microstructure while peened samples shows no visual cracks, voids. Microhardness values was taken on different zones and result shows that Microhardness value was higher in fusion zone than heat affected zone. Heat affected zone has higher hardness than base metal. Corrosion resistance of peened samples was greater than unpeened samples. Fatigue life value of peened samples were greater than unpeened samples. There was 120% increase in 300 MPa, 70% increase in 330 MPa dynamic loading range. Increase in fatigue life was due to compressive residual stresses induced during ultrasonic peening.

Kim (2013) studied the effect of air blast treatment on as welded and blast treated longitudinal fillet welded joints of KS SM400A, KS SM490B, KS SS400 (Rolled H-Beam). The fatigue test was carried on three different areas that were uniaxial tension, out of plane bending, in-plane bending stress cycles. The blasting treatment used was steel abrasive of 1 mm dia. at 0.6-0.7 MPa. Near the weld toes of blast treated joints, Compressive Residual Stresses increases by 50-300 MPa. A total of 66% increase in fatigue limit was observed at fatigue strength of 10 million cycles as compared to welded joints. At 2 million cycles fatigue strength, fatigue limit increases by 9%.

There was 6% less stress concentration in blast treated joints as compared to as weld joints. Increment of 15-40% was observed in mean weld toe radii of blast treated joints.

Akinlabi et al. (2013) studied the effect of sand blasting on mild steel sheets. The base metal was also formed by two different techniques: mechanically formed through roller of power 20 ton and laser formed using 120 mm curvature at 1.9 m/min speed, beam dia. of 12 mm, power 1.7 KW, and 25% beam overlap. To cool the irradiated material argon gas was used. Sand blasting was done using Silicon Carbide (SiC) on base metal, mechanically formed and laser formed samples. Hardness was tested at various points taking gap of 0.5 mm and average was taken. Increase in hardness after sand blasting as 44.7%, 50%, 68.2 % in base metal, mechanically formed, laser formed respectively. There was visual grain elongation in the microstructure after sand blasting. Increase in grain size was 34.3%, 62.2%, 72.4% in base metal, mechanically formed and laser formed respectively. Ultimate tensile strength changes (MPa) from 296 to 396 in base to 480 in mechanically formed, 487 to 511 in laser formed samples.

Tsujikawa et al. (2013) described Modifications of S phase on austenite stainless steel using fine particle shot peening. The specimen were AISI 304 and 316 of dimension 50 × 5 × 5 mm. Specimen was solution treated at 1030^{o} for 2.7 ks. Then they were grounded and polished to a mirror surface finish. Shot peening was done using two fine particle of Silica glass beads and Zirconia glass beads with air pressure 0.1-0.9 MPa. The peening time and distance from nozzle to specimens were 10s and 100mm. Surface roughness was increased heavily due to Zirconia glass beads but roughens less due to Silica glass beads. Zirconia beads increases hardness upto depth of 60 µm while Silica beads increases hardness only upto 20 µm. The effect of shot peening was greater in AISI 316 rather than AISI 304.

Byrne et al. (2013) described comparison between shot peening and abrasive blasting processes as deposition methods for hydroxyapatite coatings onto a titanium alloy. A Ti-6Al-4V titanium alloy (grade 5) was used as substrate. Hydroxyapatite powder with a particle size of 25-60 µm was used. Alumina abrasive (100 µm) and silica shot peening media (100 µm) with dual nozzle system with max height of 41 mm and min height of 15 mm was used. High coverage when the nozzles were closer to substrate surface. Surface roughness of silica beads was way less than alumina. Alumina surface has better adhesion than silica beads due to mechano-chemical bonding with

better inter-locking No evidence of significant shot peen silica or alumina abrasive incorporation in hydroxyapatite coating.

Sledz et al. (2013) investigated the effect of pneumatic shot peening on perforated steel sieves of different steel grades. 1 mm thick steel sieves of 4 different grades was taken: 1.0530, 1.4301, 1.8159 and 30HGSA. Pneumatic shot peening was done on both sides. Uniaxial tension test and rotational bending test was done to find out the fatigue life. Shot peening shows increment in fatigue strength of the sieves. Tensile test was done using specimen size of 250 mm gauge length and 12.5 mm width. Ultimate tensile strength increases with shot peening while elongation of the material decreases. It has no visual effect on anisotropy of the metal.

Salman et al. (2015) investigated the effect of shot peening on AA 6061-T6. 6 mm thick plates of AA 6061-T6 was butt welded using TIG welding using Argon as shielding gas. Welding parameters chosen were 90 A as welding current, 20 V as welding voltage, 120 mm/min as welding speed and 20 l/min as gas flow rate. Friction stir welding was done counter clockwise at 1000 rpm, welding speed of 50 mm/min and power of 11 Kw. Samples tested at different conditions: as received, as received + shot peened, TIG welded, TIG welded + shot peened, Friction stir welded, Friction stir welded + shot peened. Shot peening was done using steel balls of dia. 0.9 mm at angle of 90°. Higher strength values was found after friction stir welded and TIG welded. Increase in strength value were 46.3% and 33.6% for friction stir welding and TIG welding respectively. 11.5% and 4% increment in tensile strength of friction stir welded and TIG welded respectively. There was also visible value of increment in surface hardness.

2.3 Gaps Identified in the Literature Review

Literature review reveals that a substantial amount of work on effect of abrasive blasting on Aluminum has been reported. However, applicability of abrasive blasting on steel is still at the infant stage and has a long way to go. On the basis of literature review, following gaps in the literature have been identified:

1. Most of the work is associated with investigating effects of abrasive blasting on friction stir welded joints but less work is done on fusion welded joints.
2. Maximum work has been done to find out the effect of abrasive blasting on fatigue life but less work has been reported on finding out the effect on ultimate tensile strength.
3. Very less work has been reported on optimizing the time period of blasting and their effects on different fusion welded joints.
4. Not as much of work has been done on exploring out the effect of various times of blasting on tensile strength and microhardness of the material.

2.4 Objectives

On the basis of literature review and gaps found in the study following objectives have been selected.

i. To study the effect of Abrasive Blasting on low carbon steel and medium carbon steel.
ii. To find out the effect of abrasive blasting treatment on tensile strength of fusion welded joints.
iii. To investigate microhardness on fusion welded joints at different abrasive blasting time periods.
iv. To investigate the microstructure of welded structure due to abrasive blasting
v. To carry out study on fractured surface of different welded joints.

CHAPTER 3

Methodology

The proposal for present study was carried out by finding gaps in the literature review. In this present study two different steel are taken: low carbon steel and medium carbon steel, then the workpiece are welded by four different welding processes: MMA, MIG, TIG and SAW and finally workpieces are abrasive blasted at four different time periods: 10 min, 150 min, 20 min and 25 min. Different mechanical properties are tested on as welded and after abrasive blasting treatment: Microhardness, tensile strength and difference in the microstructure properties. The size of plate welds for both low carbon steel and high carbon steel is 100 × 50 × 6 mm for MMA, MIG, TIG and 100 × 50 × 12 mm for SAW.

3.1 Material and Welding Procedures

3.1.1 Material

Two different materials are used i.e. low carbon steel and medium carbon steel which was received from Bharat Aerospace metals, Mumbai.

- AISI 1018- It is a low carbon steel which is suitable for welded, riveted, bolted structures and for general engineering purposes. Chemical composition is tested by atomic absorption spectroscopy and is given in Table 3.1. Tensile strength is tested by universal testing machine and its values are given in Table 3.2.

Table 3.1- Chemical Composition of AISI 1018

Fe	C	Mn	S	P	Si
99%	0.18%	0.72%	0.040%	0.040%	0.014%

Table 3.2- Mechanical Properties of AISI 1018

Yield Strength	370 N/mm^2
Ultimate Tensile Strength	440 N/mm^2
Elongation	15%

- EN8- It is an unalloyed medium carbon steel which is used for making shafts, studs, bolts, connecting rod, screws, and rollers. Chemical composition is tested by atomic absorption spectroscopy and is given in Table 3.3. Tensile strength is tested by universal testing machine and its values are given in Table 3.4

Table 3.3- Chemical Composition of EN8

Fe	C	Mn	S	P	Si
98.19%	0.39%	0.97%	0.045%	0.050%	0.35%

Table 3.4- Mechanical Properties of EN8

Yield Strength	465 N/mm^2
Ultimate Tensile Strength	550 N/mm^2
Elongation	16%

3.1.2 Welding Procedure

Two different materials i.e. low carbon steel and medium carbon steel was received from Bharat Aerospace metals, Mumbai. Dimension of the workpieces are given below in the Table 3.5

Table 3.5: Workpiece Dimensions

Serial no.	Welding Machine	Dimension (in mm)
1	MMA, MIG, TIG	100 × 50 × 6
2	SAW	100 × 50 × 12

Workpiece surface is cleaned to remove rust, contaminants and other foreign particles because impurities tend to make the joint weaker as the welded portion is filled with gas and slag inclusions and the cohesion between metal is poor. Single-V edge with a groove angle of 45° is prepared as shown in fig. 3.1 and 3.2. Workpiece are clamped so as to fix their position then they are tacked at the back side in butt welding position so as to temporarily hold the pieces together.

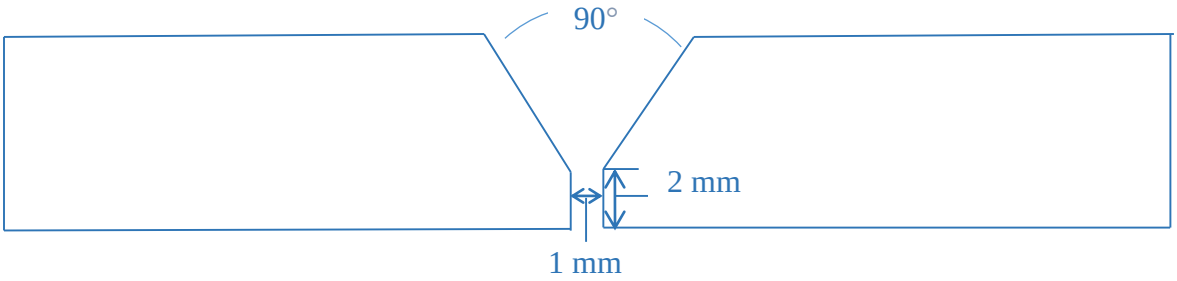

Figure 3.1-Sample for MIG, TIG, MMA Welding

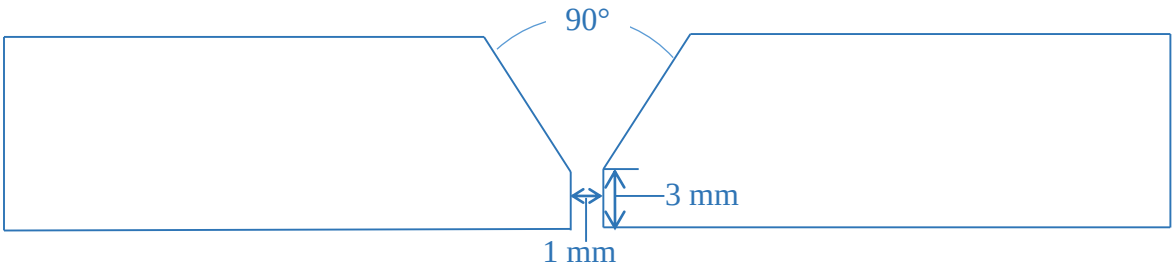

Figure 3.2-Sample for SAW Welding

3.1.3 Welding Equipments:

Four types of welding was done:

- MMA
- MIG
- TIG
- SAW

- **MMA:** It is a manual metal arc welding which uses flux coated consumable electrode. The electric source of supply can be A.C. or D.C. depending upon the requirement. Welding machine used for this purpose is available in workshop lab, Thapar University, Patiala as shown in fig. 3.3 and its specifications are given in Table 3.6.

Table 3.6: MMA welding machine specifications

Serial No.	Parameters	Range
1	Welding current	60-400 A
2	Welding voltage	20-25 V

Figure 3.3: Manual Metal Arc Welding Machine

- **MIG:** It is also known as Gas metal arc welding (GMAW). It is usually performed by using direct reverse polarity as it gives both cleaning action and fast filler metal deposition rates. It uses consumable electrode which is fed through the electrode holder into the arc, and at the same speed the electrode is melted and deposited in the weld. CO_2, Argon and mixture of argon and CO_2 can be used as a shielding gas. Welding machine used for this purpose is available in workshop lab, Thapar University, Patiala as shown in fig. 3.4 (a) and its specifications are given in Table 3.7

Table 3.7: MIG welding machine specifications

Serial No.	Parameters	Range
1	Welding Current	100-400 A
2	Welding Voltage	20-40 V
3	Gas Flow Rate	10-25 L/min

- **TIG:** It is also known as gas tungsten arc welding (GTAW). It uses inert gas which helps in keeping contaminants away from contacting the metal, and also to remove the contaminants from the metal surfaces as contaminants reduce the weld quality considerably. It uses a non- consumable electrode and a separate filler metal with an inert

shielding gas. Welding machine used for this purpose is available in workshop lab, Thapar University, Patiala as shown in fig. 3.4 (b) and its specifications are given in Table 3.8.

Table 3.8: TIG welding machine specifications

Serial No.	Parameters	Maximum value
1	Welding Current	50-400 A
2	Tungsten Electrode Diameter	1-3 mm
3	Gas Flow Rate	10-25 L/min

(a) (b)

Figure 3.4: (a) MIG and (b) TIG Welding Machine

- **SAW:** It is an automatic process developed primarily for the production of high quality butt welds in thicker steel plates. In SAW, a blanket of fusible granular material is used for shielding the arc and molten metal. The deposition rate is high and penetration is deeper. Welding machine used for this purpose is available in workshop lab, Thapar University, Patiala as shown in fig. 3.5 and its specifications are given in Table 3.9.

Table 3.9: SAW welding machine specifications

Serial No.	Parameters	Maximum value
1	Welding Current	150-1200 A
2	Welding Voltage	22-35 V
3	Travel Speed	20-600 m/h
4	Electrode Diameter	2.4-6 mm
5	Wire Feeding Rate	0.5-2.5 mm/min

Figure 3.5: Submerged Arc Welding Machine

3.2 Welding Parameters Selection

A pilot study is carried out after extensive study on literature to identify value of current and voltage on both low and medium carbon steel. Literature review suggest that current was to be varied between 100-300 A and voltage for 22-26 V for quality welding. So initially a weld bead is formed at 100 A and 20 V without use of any filler and then raised in steps of 50 A and 2 V till 250 A and 26 V. The main purpose of carrying out such study is to find out the penetration of heat energy on the down side of the plate. To find out the penetration workpiece is cut in half, grinded on belt, polished using various grades of emery paper and then etching is done with 2% nital solution. On the basis of pilot study the parameters in the range of 150 A and 22 V is selected as process parameter for welding For MMA, MIG and TIG. As per literature review gas flow rate must be varied between 6-16 L/min and included angle for butt weld joint to be varied within 60-90° for quality weld. The selection of process parameters within this range gives best possible results. Gas flow rate affects the finished weld penetration, depth, surface profile, composition, porosity, corrosion resistance, strength, ductility, hardness and brittleness. Gas flow rate is taken 16 L/min and groove angle of 90° is selected. Similarly same process is done for SAW welding process and it was found that optimal solution comes in the range of 32 V and 350 A. For MIG, TIG and MMA welding same range of parameters has been selected so that different results can be compared to each other, but in case of SAW welding high thickness plate is required so same parameter cannot be applied to SAW because it can cause weld defects like incomplete penetration etc.

3.3 Abrasive Blasting Period

Selection of time period is done on the basis of literature gap and future scope, so as to optimize the time period of blasting. The different time period for Abrasive blasting taken are 10 min, 15 min, 20 min and 25 min.

3.4 No. of Experiments

According to the different welding to be done and abrasive blasting time period, there are 20 experiments to be done on each material. So total of 40 experiments needs to be done as shown in Table 3.10

No of welding: 4

Abrasive blasting time period: 5 (counting 0 min)

Total experiment for each material: 20

No. of materials: 2

Total experiments: 40

Table 3.10: No. of experiments to be performed on each material

SR. NO.	Name	Shot blasting time period
1	ARC	0
2	ARC	10
3	ARC	15
4	ARC	20
5	ARC	25
6	MIG	0
7	MIG	10
8	MIG	15
9	MIG	20
10	MIG	25
11	TIG	0
12	TIG	10
13	TIG	15
14	TIG	20
15	TIG	25
16	SAW	0
17	SAW	10
18	SAW	15
19	SAW	20
20	SAW	25

3.5 Welding of Carbon Steel Plates

3.5.1 Edge preparation of specimens

In common welding practices, the welding surface needs to be prepared to ensure the strongest weld possible. Preparation is needed for all forms of welding and all types of joints. Filler metal, in the form of welding rod or wire is always used in making V-butt welds. It is seldom possible to make a satisfactory, full strength weld by merely butting the pieces tight together, without spacing and then melting the edges together. So edges must be properly prepared by cleaning it with wire brush or grinder so as to provide a rust free and clean environment surface thus ensuring stronger weld.

3.5.2 Welding of specimens

The welding of carbon steel specimens are carried out as per no. of experiments to be performed with all necessary precautions and the pieces are cooled naturally in open air. The Fig. 3.6 and 3.7 shows different welded pieces on different welding machines.

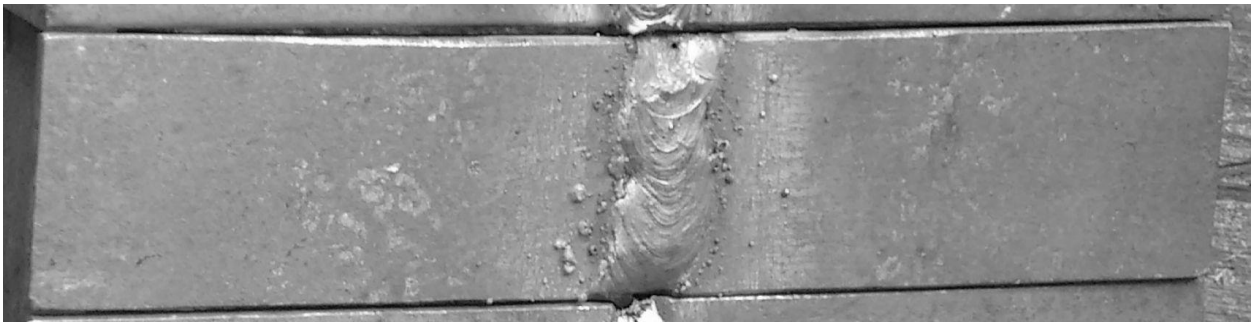

(a)

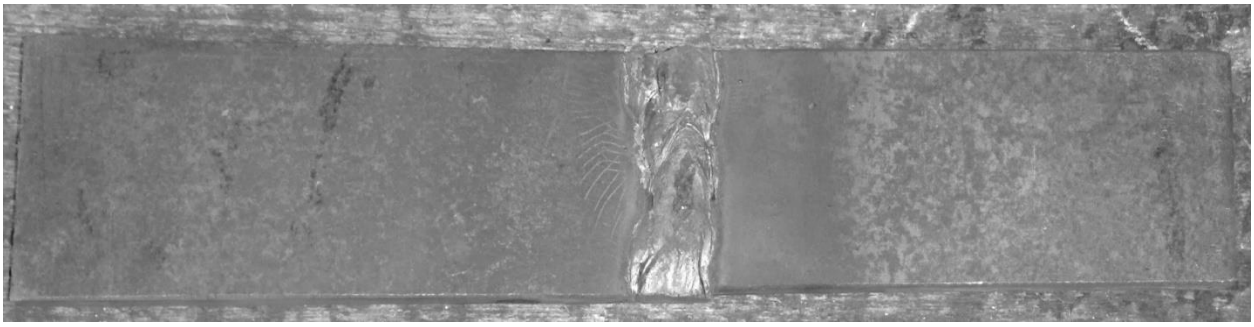

(b)

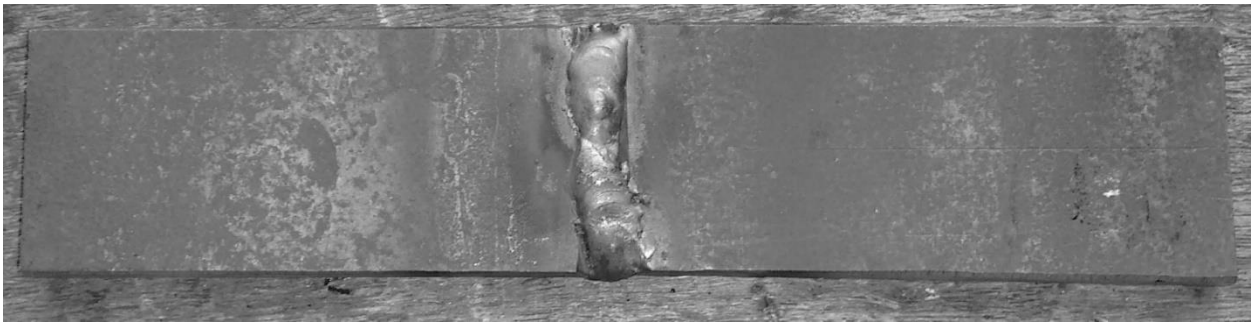

(c)

(d)

Figure 3.6: Specimens of low carbon steel with different welding techniques
(a) MMA (b) MIG (c) TIG (d) SAW

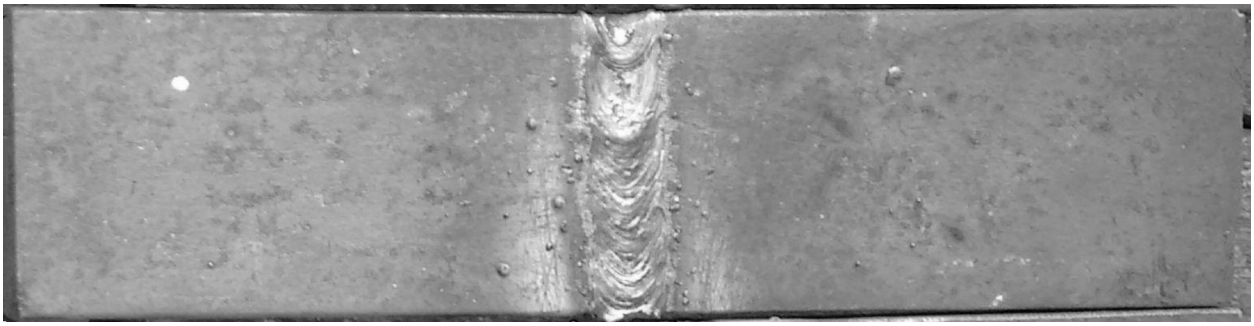

(a)

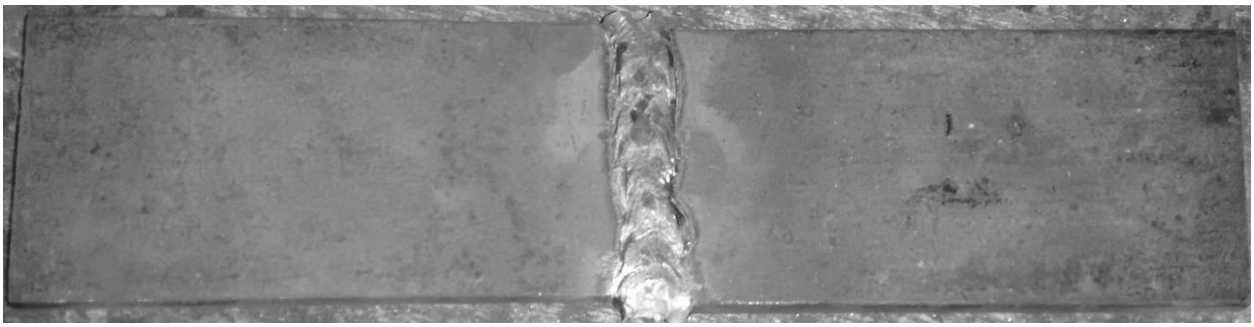

(b)

(c)

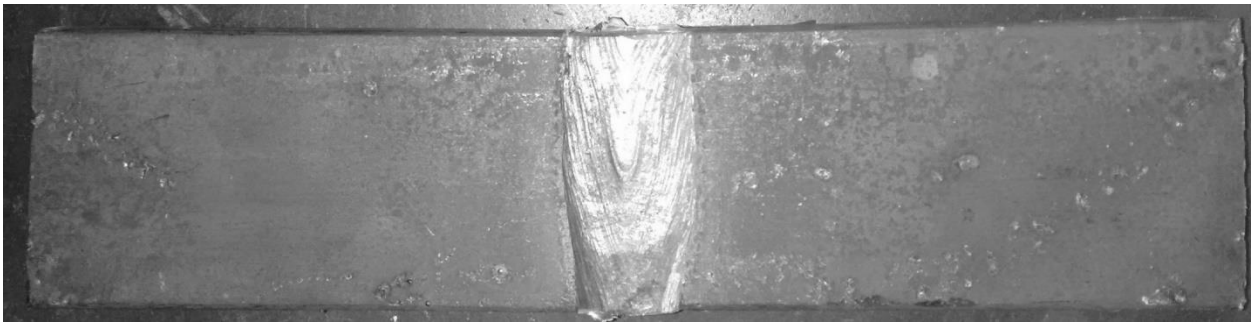

(d)

Figure 3.7: Specimens of medium carbon steel with different welding techniques
(a) MMA (b) MIG (c) TIG (d) SAW

3.5.3 Cutting of welded specimens for various testing

The following figure shows the plan according to which welded specimens are cut using hand grinder. A margin of 2 mm is already included during cutting of specimens. The specimens were grinded to make them of exact sizes.

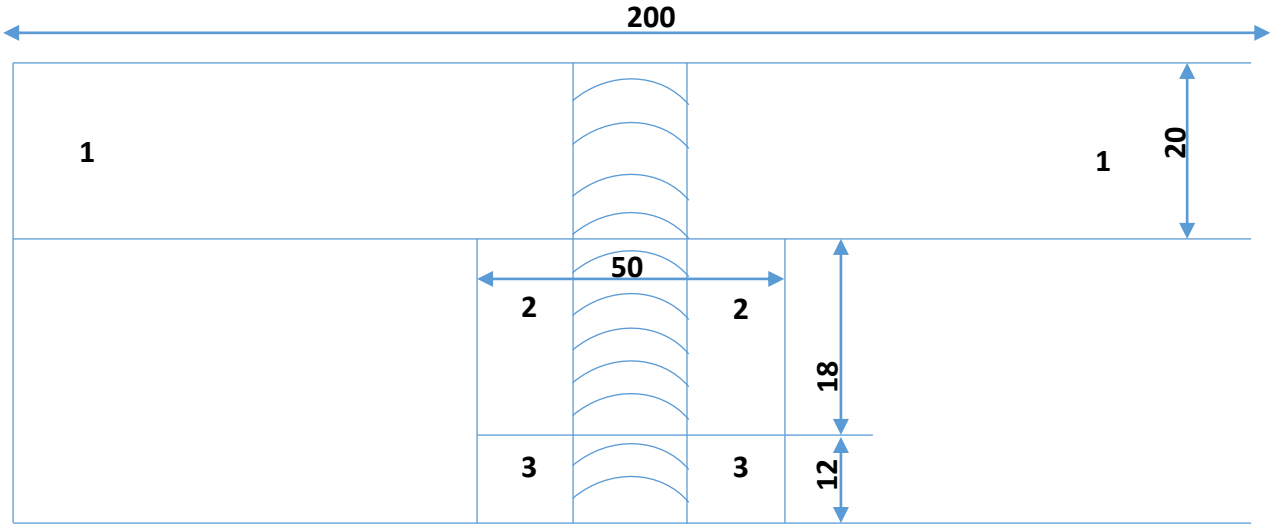

Figure 3.8: Marking and cutting plan of welded specimens (all dimensions in mm)

Table 3.11: Description of various marked positions for both low carbon and medium carbon steel

Marking on welded specimen	Usage for particular test measurement
1-1	Specimen for Tensile Testing
2-2	Specimen for chemical composition of weld bead
3-3	Specimen for microhardness and microstructure

3.6 Work Plan

The following fig. 3.9 shows the flow chart of work plan.

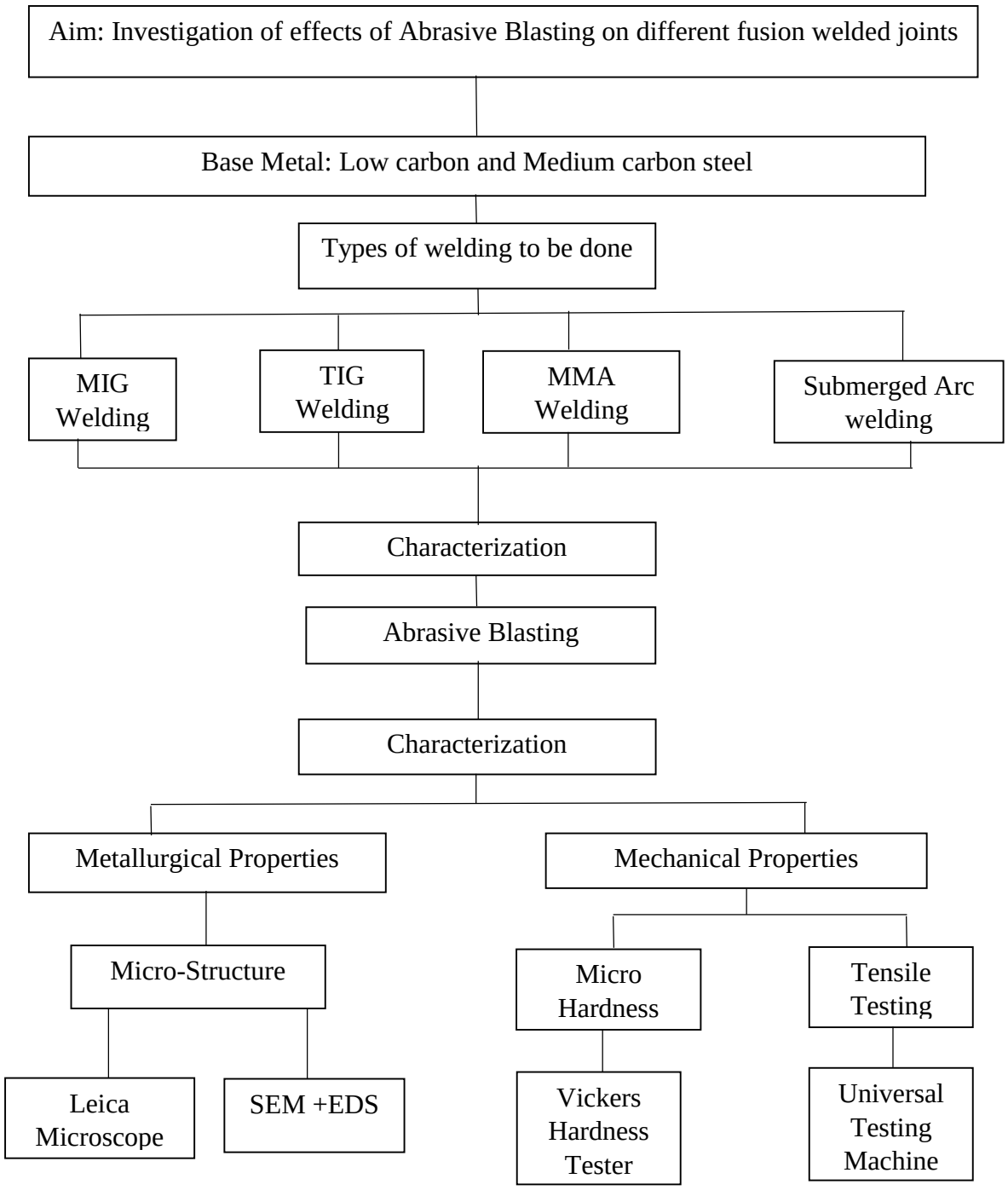

Figure 3.9: Flow chart of work plan

3.7 Metallographic Analysis

Welding samples are to be prepared for metallographic analysis. The FW joints were cross-sectioned into 50 mm × 10 mm samples, which are grinded and mechanically polished with master disc grinder polisher with coarser silicon carbide paper shown in fig. 3.11. Next the samples are polished with the help of finer grade silicon carbide paper until scratch free and mirror like finish is obtained. To reveal the microstructure of the weld it is etched with 2% natal solution and further cleaned with acetone. Then the microstructure is revealed with the help of Leica microscope shown in fig. 3.10.

Figure 3.10: Leica Microscope available at Thapar University

Figure 3.11: Master Disc Polisher Grinder

3.8 Chemical Composition

Atomic absorption spectroscopy (AAS) is an analytical technique that measures the concentration of elements. Atomic absorption is so sensitive that it can measure down to parts per billion of a gram in a sample. The technique makes use of the wavelengths of light specifically absorbed by an element. They correspond to the energies needed to promote electrons from one energy level to another. Atomic absorption spectroscopy has many uses in different areas of chemistry.

In AAS the atomized sample is converted into ground state free atoms in the vapour state and abeam of electromagnetic radiation emitted from excited lead atoms is passed through the vapourised sample. Some of the radiation is absorbed by the lead atoms in the sample. The greater the number of atoms there is in vapour, the more radiation is absorbed. The amount of light absorbed is proportional to the number of lead atoms. Spectroscopy is the study of matter and its properties by the use of spectra. Each chemical element, when heated so that it gives off light, yields a different series of lines in a spectrum. The position of the lines and the patterns they form in the spectrum of a particular substance can yield many kinds of information about the substance.

Spectroscopy is not limited to the visible-light spectrum, but includes the spectra of other forms of electromagnetic radiation, such as X-rays, infrared radiation and radio waves. The surface of specimen should be free from contaminants and polished. Now a source of light is required which emits light towards a source of heat flame or spark. The source of heat comprises of vapourised atoms of metal surface being analysed in ground state. There is absorption of some part of light during the process. This is passed through a focusing lens and then on the prism which further divide the light into different sections. This is then aimed on to a device called photomultiplier which provide us the reading. It is with the help of Atomic emission spectroscopy, we can analyse the types of alloying elements but to know their composition, AAS principle is used.

The chemical composition of base metal and welded bead was found by making use of AAS (Make: Foundry Master) as shown in fig. 3.12. The software named Worldwide Analytical System was used by the interface which tells about chemical composition. The argon gas was discharged at the flow rate of 60 L/min for forming a shielding atmosphere during the time sparking occurs between specimen and electrode during finding out the chemical composition.

Figure 3.12: Atomic Absorption Spectrometer (Model: DV-6), Baird, USA

3.9 Microhardness Test

Microhardness usually used for soft material or such material where we cannot apply high load. The term microhardness testing usually refers to static indentations made by loads of 1kg or less. It is available in mechanical department, Thapar University, Patiala as shown in fig. 3.13. In this machine, we can vary load from 50 g to 1 Kg. The work piece which hardness is to be measured is put under microscope. Then load is applied to the work piece. There is a dwell time up to which indenter indent on the surface of work piece. The shape of the tool is square pyramid and it is made of diamond. After the load is removed, the indentation is watched in the desktop attached to it. In the desktop, there is 'Quantimet' software which is used to calculate the hardness value. First the software needs to be calibrated. The plate which hardness needs to be measured must be properly cleaned and polished so that there should not be any scratch on indentation. After calibration, load is defined in software and four ends of the square indentation are selected. The software automatically calculates the dimensions of indentation and corresponding Vickers hardness value. For getting an indentation, load applied to indenter is 500 grams for 20 seconds dwell time.

(a)

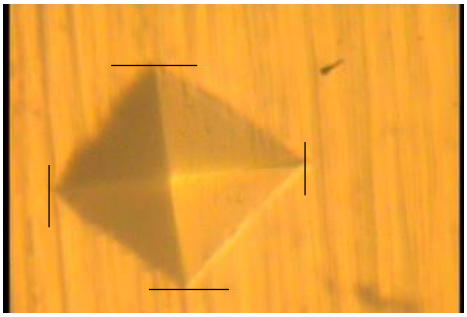

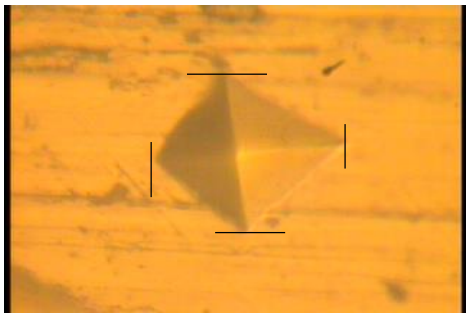

(c)

Figure 3.13: (a) Microhardness Tester (Model: MVH-2), (b) Indentation on low carbon steel and (c) Indentation on medium carbon steel

3.10 Sample Design and Preparation of Tensile Test

The basic test for determination of material behaviour is the tensile test. A specimen is ruptured by a test machine while the actual force and the elongation of the specimen is measured. With these measurement values, tension σ and strain ϵ are calculated. Normally, if steel with a bcc lattice structure is tested, a curve with a clear yield point is obtained. Steels with an fcc lattice structure show a curve without yield point. Tensile test specimen has enlarged ends or shoulders for gripping. The important part of the specimen is the gauge section. The cross-sectional area of the gauge section is reduced relative to that of the remainder of the specimen so that deformation and failure will be localized in this region. The gauge length is the region over which measurements are made and is centred within the reduced section. The tensile test is performed on all the specimens for both materials. The shape and size of the specimen chosen is in accordance with ASTM specification E8 as shown in figure 3.14.

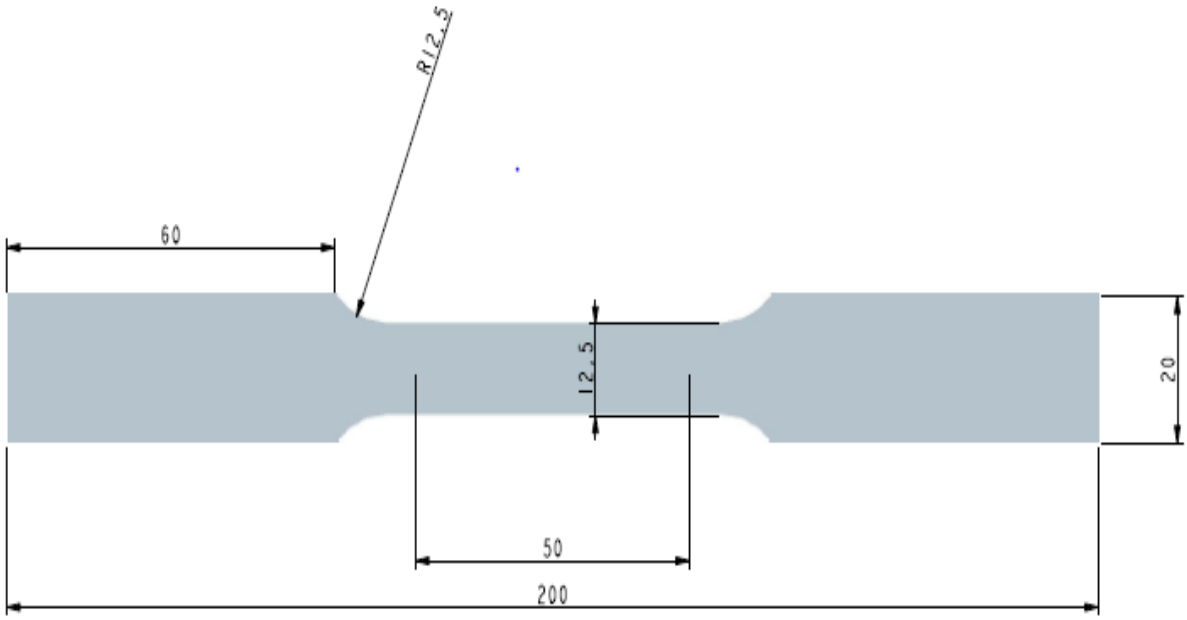

Figure 3.14: Tensile specimen according to ASTM E-8 (all dimensions are in mm)

Twenty samples are prepared from both carbon steel, one for each welding and corresponding to period of shot blasting. Tensile test is carried out at Guru Granth Sahib World University, Fatehgarh Sahib taking strain rate as 1mm/min as shown in figure 3.15. The universal testing machine (TUE-C-1000-SERVO) is used to carry out the tensile tests of different materials. It has a capacity of 1000 kN, provided with different fixtures for tensile and flexural testing. This

machine has maximum allowable elongation of 250 mm. It has electronically sophisticated imported pressure and flow control valve with dedicated controller which is used to provide desired loading and strain rate. The loads and strain rate are provided with computer attached to the machine. It has DAS panel with 32 bit micro controller system which can be connected to different computer systems. It has load accuracy as high as ± 1% of machine capacity. The machine satisfies IS: 1828 and BS: 1610 standards.

Figure 3.15: Universal testing machine

(Courtesy; Guru Granth Sahib World University, Fatehgarh Sahib)

3.11 Abrasive Blasting Procedure

Abrasive Blasting is done with the help of tumbling-blast machine model ATB (Automatic Tumble Blast) by MEC Shot Blasting equipments, INDIA as shown in figure 3.16. It consists of an enclosed, endless conveyor belt, a centrifugal blast wheel and an abrasive recycling system. These machines simultaneously tumble and blast the work pieces. As the conveyor moves, it gently tumbles the work and exposes all work piece surfaces to the abrasive system.

3.11.1 Specifications of abrasive blasting machine:

- **Working chamber**

  Length× width× height: 1360×1500×1600 mm
- **Sliding door**

  Width× height: 750×700 mm

  Liners: 6mm thick manganese Liners
- **Belt tumbler**

  Belt size: 1320×4925×17 mm

  Belt drive motor: 1 HP
- **Bucket elevator**

  Motor: 1 HP

  Elevator bucket: 10×100×7688 mm

  No. of buckets: 32
- **Dust collector**

  Blower capacity: 1200 CFM

  Motor: 3 HP

  Filter bags: 24 Nos.
- **Blast wheel unit**

  Size of blast wheel: 12.5” × 2.5”

  Motor for blast wheel: 7.5 HP

3.11.2 Blasting material:

Round steel shots, Size = 0.425mm size, Grade = S170

Chemical composition = carbon 0.6 to 1.25%, silicon 0.2 to 1.1%, manganese 1.25% max., sulphur 0.08% max., phosphorous 0.08% max.

Figure 3.16: Automatic tumble blasting machine (ATB)

3.12 Fractographic Analysis

Fractography is used to study the fractured surface of the material. Main aim of fractography is to find out the origin of cracking as it may help in failure analysis or product failure. To evaluate theoretical models of crack growth behaviour in material science fractography is used. The scanning electron microscopy (SEM) is used to view the structure at different ranges. In this an electron beam is passed to the work piece then secondary electrons are emitted from the plate. Fractography of the surface can be observed by electron probe over the surface and acquisition of an image from the detected secondary electrons. This SEM (Make: JSM-6510LV, JEOL Ltd, Tokyo, Japan) is available at SAI Labs, Thapar Technology Campus, Patiala. SEM analysis is a "non-destructive" test because the fine electron beam doesn't leads to the loss in the volume from the work piece surface. It is a high performance and low vacuum SEM for fast characterization and imaging of fine structures and has a magnification range 5–300,000 X. For this, a high vacuum is required, because electron should be focused on the particular zone, so a high vacuum is created inside the box of the machine. This machine is connected with EDS in which phase composition can be observed. The image of SEM+EDS is shown in figure 3.17.

Figure 3.17: Scanning electron microscope + Energy dispersive spectroscopy
(Courtesy; SAI Lab, Thapar University, Patiala)

Chapter 4

Results and Discussion

4.1 Introduction:

The previous chapter focused on the basis of carrying out preliminary experimentation to find out the selecting parameters required for welding and abrasive blasting. According to parameters found in the investigation the experimental setup was prepared and various equipments required for experimentation was analysed. This chapter focuses on the experimentation based on above data and investigating the various results of the experiments. Table 4.1 to 4.8 shows the VHN profiles of different fusion welds on low carbon and medium carbon steel. Table 4.9 to 4.16 shows the tensile strength of as welded and abrasive blasted joints of low carbon and medium carbon steel. Then fractography and microstructure of different joints were analysed.

4.2 Results of Microhardness Test

Microhardness was carried out on fusion welded joints using Vickers Hardness on low carbon steel and medium carbon steel. Microhardness profiles were carried out by taking microhardness values at various points: at fusion zone, heat affected zone and base metal. The points were selected according to the weld penetration and its width which was checked after cross-sectioning the piece, polishing it with various emery papers and then etching it with 2% nital solution. The weld beads penetration and its width affects the distance of points from plate joint line (PJL). In MMA, MIG, TIG average weld width was 4 mm in each direction from PJL and in SAW it was 10 mm in each direction from PJL. So Point 3, 4 and 5 shows the hardness values at fusion zone according to the weld width. Point 2 and 6 shows hardness values at heat affected zone taking 2 mm distance from fusion zone. Point 1 and 7 shows the hardness values at base metal or unaffected area taking distance of at least 4 mm from heat affected zone.

4.2.1 Results of microhardness test on low carbon steel:

MMA Welding:

Table 4.1 shows microhardness values of MMA welding and fig. 4.1 shows its microhardness profiles.

Table 4.1: Results of microhardness of MMA welding on low carbon steel

Sr. No.	Time Period / Distance(in mm)	No Blasting	10 Minutes	15 Minutes	20 Minutes	25 Minutes
1	-10	155.886	178.07	195.36	201.1498	209.23
2	-6	170.378	197.5	222.54	232.451	237.651
3	-3	190.4132	214.788	239.33	251.4312	258.9872
4	0	194.9845	223.1	238.65	249.3275	257.8761
5	3	188.6433	210.792	241.95	250.3756	253.11474
6	6	169.875	195.748	219.16	231.1452	239.5862
7	10	152.3283	175.236	194.95	206.02	211.658

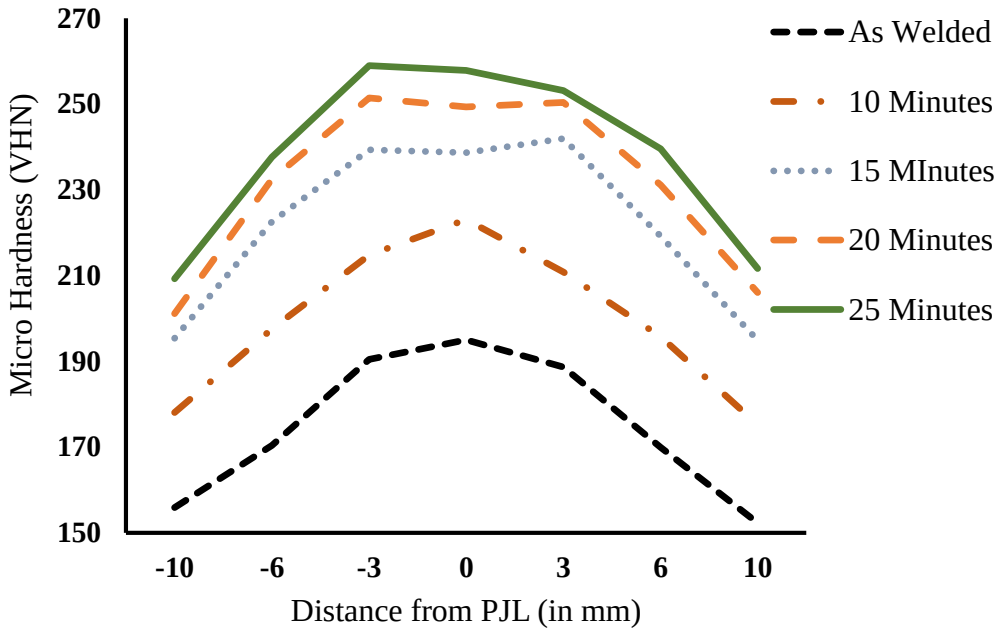

Figure 4.1: Microhardness profiles of MMA on low carbon steel

MIG Welding:

Table 4.2 shows microhardness values of MIG welding and fig. 4.2 shows its microhardness profiles.

Table 4.2: Results of microhardness of MIG welding on low carbon steel

Sr. No.	Time Period / Distance(in mm)	No Blasting	10 Minutes	15 Minutes	20 Minutes	25 Minutes
1	-10	141.0159	182.0727	196.1764	201.5896	207.994
2	-6	160.1257	201.5799	210.882	220.3587	225.8872
3	-3	185.3901	226.0168	236.1896	238.538	248.2398
4	0	187.3106	228.9616	239.7823	246.5805	250.2015
5	3	184.397	227.1265	235.1649	239.2981	248.5672
6	6	161.2148	203.0192	208.3497	216.228	221.9285
7	10	142.9124	186.7647	194.2391	202.4386	209.5539

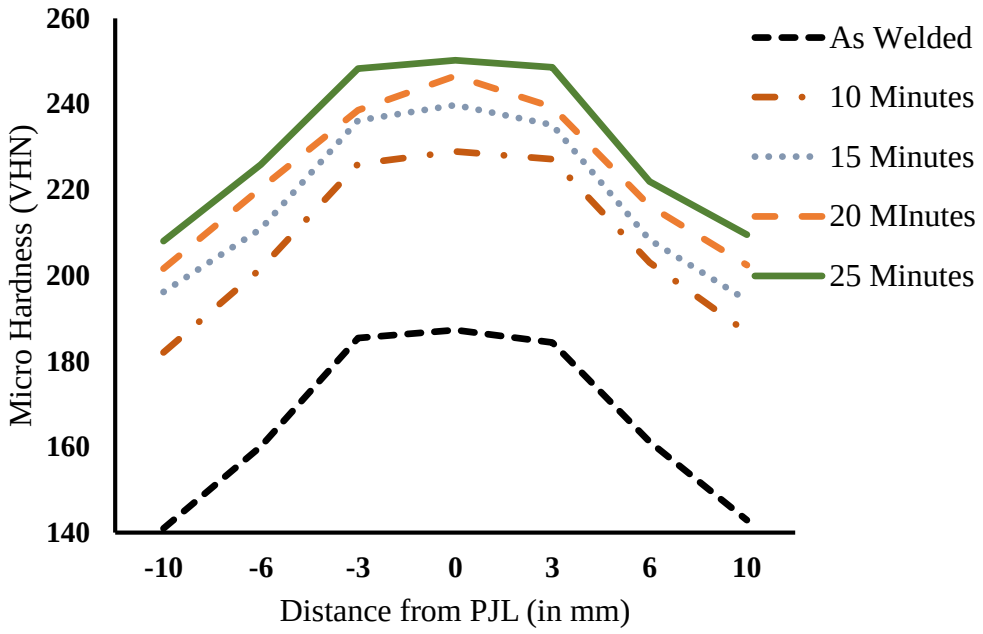

Figure 4.2: Microhardness profiles of MIG on low carbon steel

TIG Welding:

Table 4.3 shows microhardness values of TIG welding and fig. 4.3 shows its microhardness profiles.

Table 4.3: Results of microhardness of TIG welding on low carbon steel

Sr. No.	Time Period / Distance(in mm)	No Blasting	10 Minutes	15 Minutes	20 Minutes	25 Minutes
1	-10	141.2356	168.3222	192.476	201.7436	208.9461
2	-6	161.2548	191.2549	210.4678	220.4765	227.3579
3	-3	191.3222	230.9855	243.488	252.1289	260.8851
4	0	193.8116	226.8349	244.538	255.4538	262.5637
5	3	191.4975	225.4752	241.5879	251.8972	259.9778
6	6	165.489	195.4637	211.5498	218.4834	226.5589
7	10	140.2469	170.9871	188.7831	197.7895	205.5473

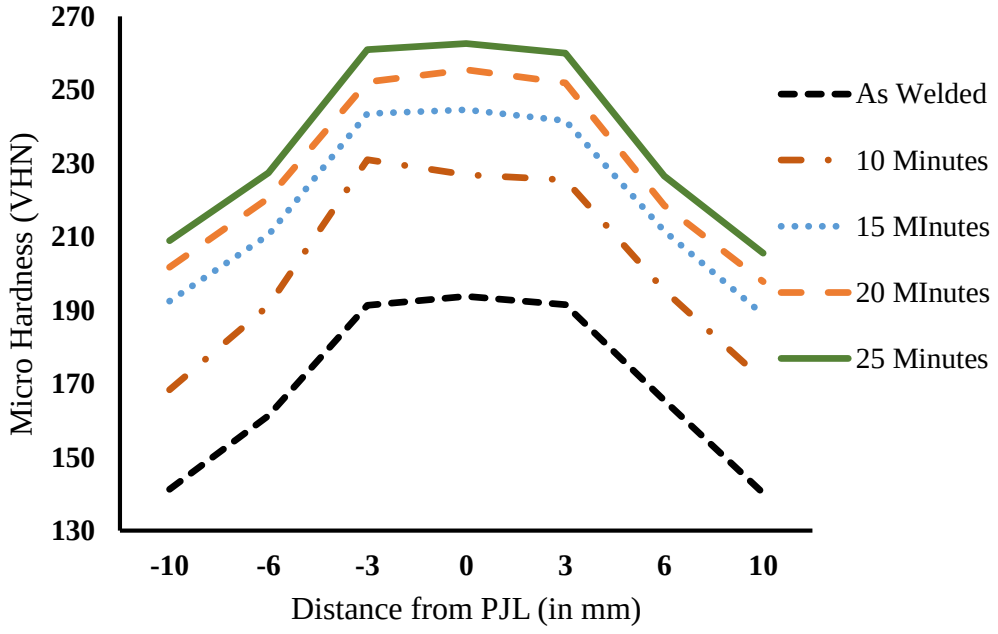

Figure 4.3: Microhardness profiles of TIG on low carbon steel

SAW Welding:

Table 4.4 shows microhardness values of SAW welding and fig. 4.4 shows its microhardness profiles.

Table 4.4: Results of microhardness of SAW welding on low carbon steel

Sr. No.	Time Period / Distance(in mm)	No Blasting	10 Minutes	15 Minutes	20 Minutes	25 Minutes
1	-18	162.439	189.558	201.5561	211.2546	219.5825
2	-12	175.794	212.558	228.632	235.5782	246.3192
3	-5	200.257	235.6873	254.0153	261.2197	268.0049
4	0	198.1685	236.4768	255.5475	262.6894	270.0331
5	5	203.716	233.7861	252.4818	264.884	271.5413
6	12	178.8256	215.8167	228.0556	236.5549	245.7505
7	18	160.553	184.5286	200.1316	212.9888	220.0168

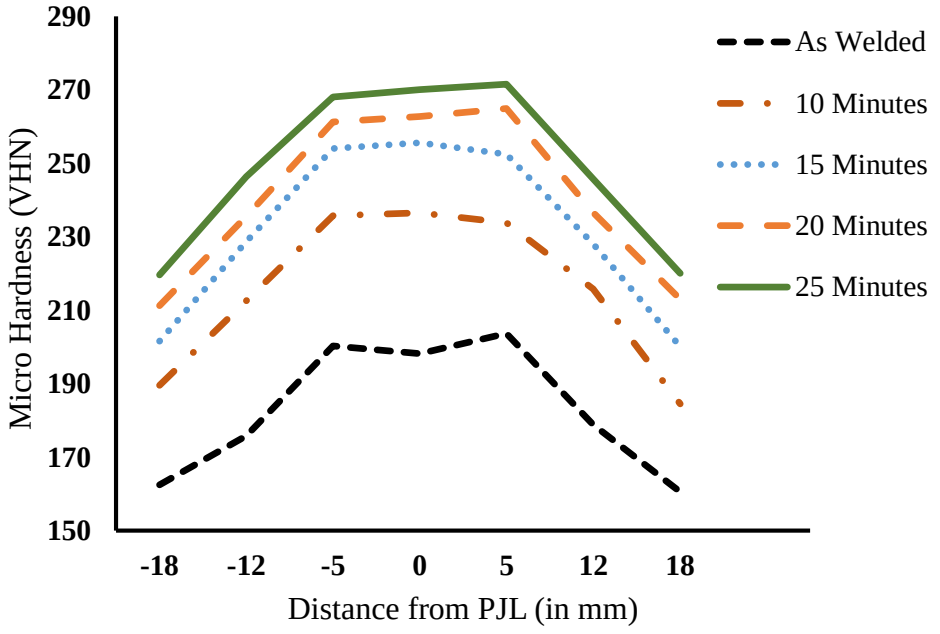

Figure 4.4: Microhardness profiles of SAW on low carbon steel

Microhardness profile shows that fusion zone has the highest microhardness value among fusion zone, heat affected zone and base metal. Heat affected zone has higher microhardness value than

base metal. Abrasive blasting treatment increases the microhardness values of welded joints. The values of microhardness considering the increasing time period of blasting shows that microhardness increases with increase in blasting time period. The increase in microhardness is due to induced plastic deformation on the surface thereby increasing internal compressive stresses of the material. In MMA welding the average value of VHN at FZ of as welded joint is 191.3486 which increases to 216.226, 239.976, 250.378 and 256.6593 after 10 minutes, 15 minutes, 20 minutes and 25 minutes of blasting treatment respectively. The average VHN values at HAZ of as welded joint is 170.1265 which increases to 196.624, 220.85, 231.7981 and 238.6186 after 10 minutes, 15 minutes, 20 minutes and 25 minutes of blasting treatment respectively. The average VHN value of base metal of as welded joint is 154.1071 which increases to 176.53, 195.115, 203.5849 and 210.444 after 10 minutes, 15 minutes, 20 minutes and 25 minutes of blasting treatment respectively. The increase in VHN values shows that time period of blasting treatment has significant effect. VHN values shows that initially there is a large increment till 15 minutes but after that there is only small increment. In MIG the average VHN values for BM are 141.9642, 184.4187, 195.2078, 207.0141 and 208.774, the VHN values at HAZ are 160.6703, 202.2996, 209.6159, 218.2934 and 223.9079 and VHN values at FZ are 185.6992, 227.3683, 237.6456, 241.4722 and 249.0028 in increasing time period of blasting treatment respectively. In TIG the average VHN values for BM are 140.743, 169.6547, 190.6296, 199.7666 and 207.2467, the VHN values at HAZ are 163.3719, 193.3193, 211.0088, 219.48 and 226.9584 and VHN values at FZ are 192.2104, 227.7652, 243.2046, 253.16 and 261.1422 in increasing time period of blasting treatment respectively. In SAW the average VHN values for BM are 161.496, 187.0433, 200.8439, 212.1217 and 219.7997, the VHN values at HAZ are 177.3098, 214.1874, 228.3438, 236.0666 and 246.0349 and VHN values at FZ are 200.1738, 235.3167, 254.0149, 262.931 and 269.8598 in increasing time period of blasting treatment respectively. The VHN values shows that SAW welding gives highest microhardness values at FZ, HAZ and BM as it has deeper penetration and there are less chances of defects because of arc submerged in flux. If we compare microhardness values among MMA, MIG and TIG, TIG has better hardness values than MMA and MIG because TIG has better shielding environment.

4.2.2 Results of microhardness test on medium carbon steel:

MMA Welding:

Table 4.5 shows microhardness values of MMA welding and fig. 4.5 shows its microhardness profiles.

Table 4.5: Results of microhardness of MMA welding on medium carbon steel

SR. No.	Time Period / Distance(in mm)	No Blasting	10 Minutes	15 Minutes	20 Minutes	25 Minutes
1	-10	170.9845	195.4275	211.4312	217.6433	225.0331
2	-6	192.6862	219.5413	235.1053	245.4857	252.0698
3	-3	211.2945	238.7408	252.488	261.5898	270.1598
4	0	213.935	237.0177	255.5805	264.4848	273.792
5	3	215.5138	235.2945	255.5343	262.1147	271.3598
6	6	195.2954	211.2867	232.0169	242.9845	250.132
7	10	166.6433	194.653	209.1147	216.4132	224.5826

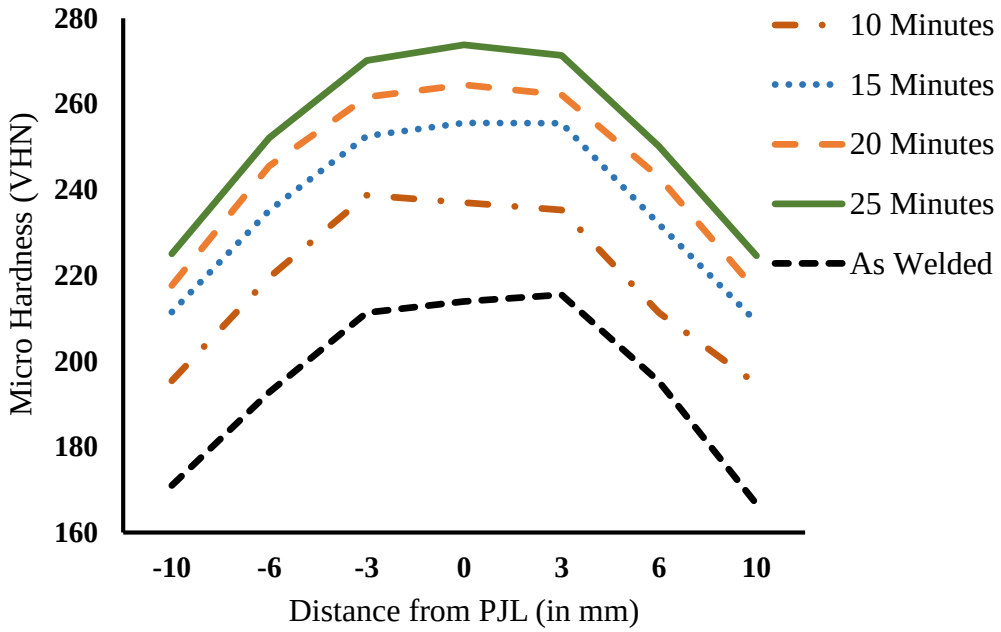

Figure 4.5: Microhardness profiles of MMA on medium carbon steel

MIG Welding:

Table 4.6 shows microhardness values of MIG welding and fig. 4.6 shows its microhardness profiles.

Table 4.6: Results of microhardness of MIG welding on medium carbon steel

SR. NO.	Time Period / Distance(in mm)	No Blasting	10 Minutes	15 Minutes	20 Minutes	25 Minutes
1	-10	165.5539	199.8872	210.5066	218.3799	226.7954
2	-6	193.6862	229.3001	239.2806	245.2802	252.4246
3	-3	217.1084	241.7284	259.4833	264.8116	271.8406
4	0	221.2954	245.7326	260.4386	268.1703	273.9485
5	3	216.9214	246.7305	259.961	265.991	270.7326
6	6	192.5873	225.4246	238.7326	245.1349	250.1662
7	10	168.1368	201.3624	215.3901	225.7647	230.5596

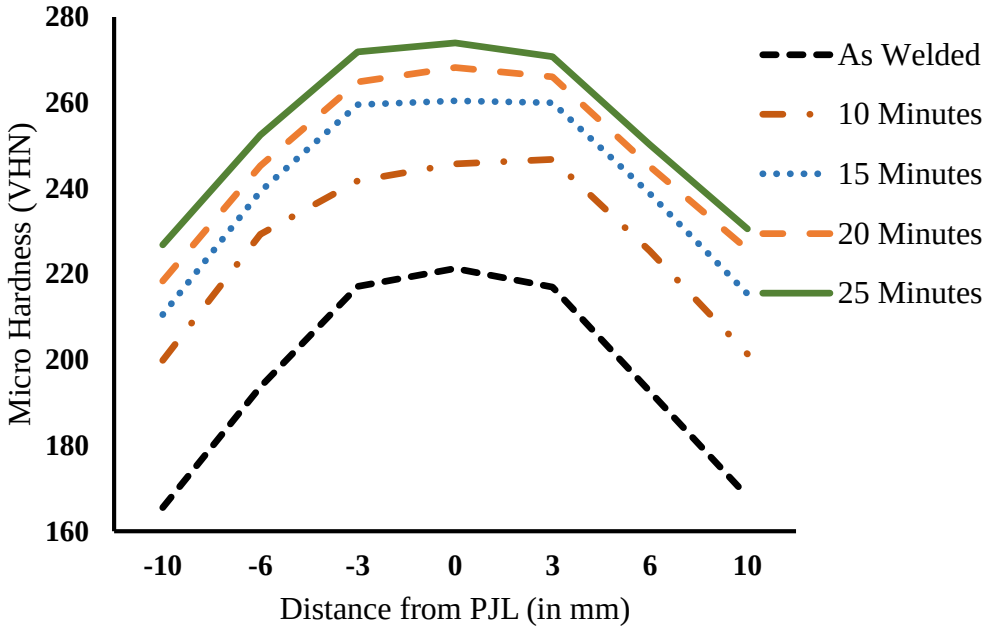

Figure 4.6: Microhardness profiles of MIG on medium carbon steel

TIG Welding:

Table 4.7 shows microhardness values of TIG welding and fig. 4.7 shows its microhardness profiles.

Table 4.7: Results of microhardness of TIG welding on medium carbon steel

SR. NO.	Time Period / Distance(in mm)	No Blasting	10 Minutes	15 Minutes	20 Minutes	25 Minutes
1	-10	161.9461	192.4765	209.0209	215.2356	224.451
2	-6	196.6622	222.1452	233.5474	240.2548	250.1962
3	-3	218.0556	248.0049	264.1962	270.9855	279.4678
4	0	216.0365	252.7349	266.0168	273.4752	280.8349
5	3	217.0461	243.0209	262.3756	275.9871	281.4766
6	6	198.2529	225.3357	235.3699	243.489	253.077
7	10	164.5498	189.4818	207.8618	216.4975	225.4411

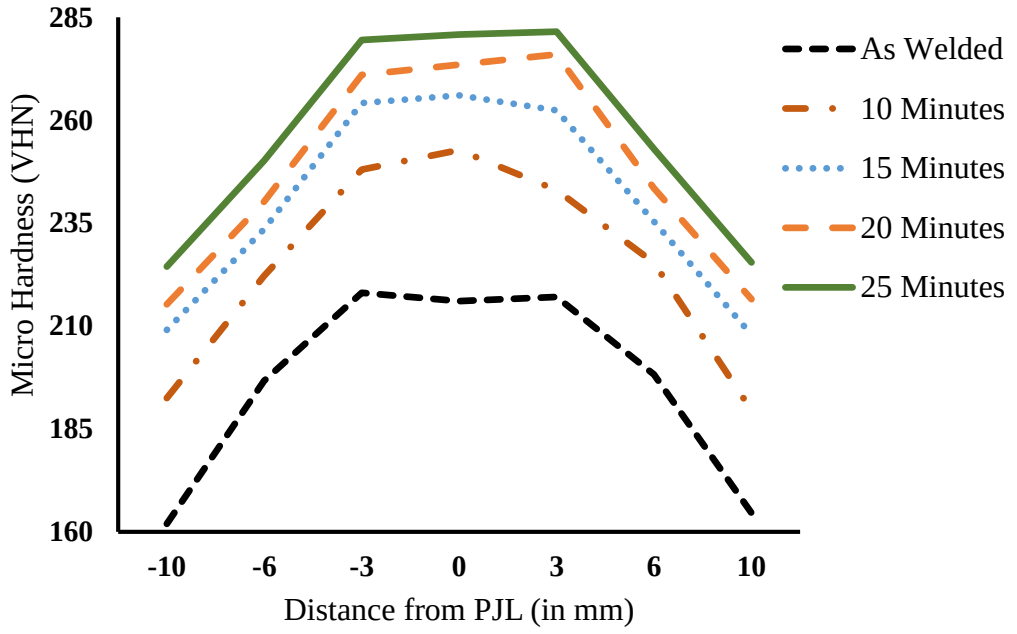

Figure 4.7: Microhardness profiles of TIG on medium carbon steel

SAW Welding:

Table 4.8 shows microhardness values of SAW welding and fig. 4.8 shows its microhardness profiles.

Table 4.8: Results of microhardness of SAW welding on medium carbon steel

Sr. No.	Time Period / Distance(in mm)	No Blasting	10 Minutes	15 Minutes	20 Minutes	25 Minutes
1	-18	181.5825	200.5782	226.6873	234.8256	240.439
2	-12	202.479	231.4573	245.1753	255.553	262.077
3	-5	216.6689	255.4573	269.5805	280.4821	288.4821
4	0	225.2954	257.0514	272.4312	281.125	290.482
5	5	218.9822	258.6455	269.0059	279.3036	286.505
6	12	201.6662	238.2148	248.4231	253.6455	261.7349
7	18	180.0168	204.2197	222.6873	230.8167	239.7992

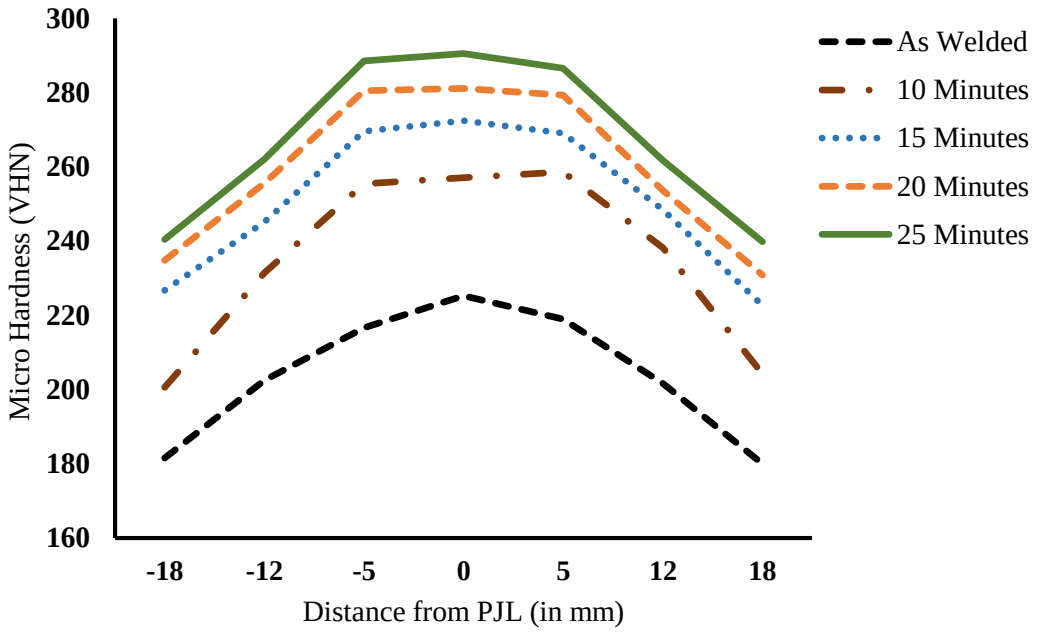

Figure 4.8: Microhardness profiles of SAW on medium carbon steel

Microhardness profile shows that fusion zone has the highest microhardness value among fusion zone, heat affected zone and base metal. Heat affected zone has higher microhardness value than base metal. Abrasive blasting treatment increases the microhardness values of welded joints. The values of microhardness considering the increasing time period of blasting shows that microhardness increases with increase in blasting time period. The increase in microhardness is due to induced plastic deformation on the surface thereby increasing internal compressive stresses of the material. In MMA welding the average value of VHN at FZ of as welded joint is 213.5811 which increases to 237.0176667, 254.5342667, 262.7297667 and 271.7705333 after 10 minutes, 15 minutes, 20 minutes and 25 minutes of blasting treatment respectively. The average VHN values at HAZ of as welded joint is 193.9908 which increases to 215.414, 233.5611, 244.2351 and 251.1009 after 10 minutes, 15 minutes, 20 minutes and 25 minutes of blasting treatment respectively. The average VHN value of base metal of as welded joint is 168.8139 which increases to 195.0402, 210.2729, 217.0282 and 224.8078 after 10 minutes, 15 minutes, 20 minutes and 25 minutes of blasting treatment respectively. The increase in VHN values shows that time period of blasting treatment has significant effect. VHN values shows that initially there is a large increment till 15 minutes but after that there is only small increment. In MIG the average VHN values for BM are 166.8453, 200.6248, 212.9483, 222.0723 and 228.6775 , the VHN values at HAZ are 193.1367, 227.3623, 239.0066, 245.2075 and 251.2954 and VHN values at FZ are 218.4417, 244.7305, 259.9609667, 266.3243 and 272.1739 in increasing time period of blasting treatment respectively. In TIG the average VHN values for BM are 163.2479, 190.9791, 208.4413, 215.8665 and 224.9460, the VHN values at HAZ are 197.4575, 223.7404, 234.4586, 241.8719 and 251.6366 and VHN values at FZ are 217.0460, 247.9202, 264.1962, 273.4826 and 280.5931 in increasing time period of blasting treatment respectively. In SAW the average VHN values for BM are 180.7996, 202.3989, 224.6873, 232.8211 and 240.119, the VHN values at HAZ 202.0726, 234.8360, 246.7992, 254.5992 and 261.9059 and VHN values at FZ are 220.3155, 257.0514, 270.3392, 280.3035 and 288.4897 in increasing time period of blasting treatment respectively. The VHN values shows that SAW welding gives highest microhardness values at FZ, HAZ and BM as it has deeper penetration and there are less chances of defects because of arc submerged in flux. If we compare microhardness values among MMA, MIG and TIG, TIG has better hardness values than MMA and MIG because TIG has better shielding environment.

4.3 Metallurgical Study

For Metallurgical study the samples were cross-sectioned, cleaned, polished and etched. The microstructure is seen under Leica Microscope. The fusion welding has three different zones. Fig. 4.9 shows microstructure of as welded joints and fig. 4.10 shows the microstructure of abrasive blasted welded joints.

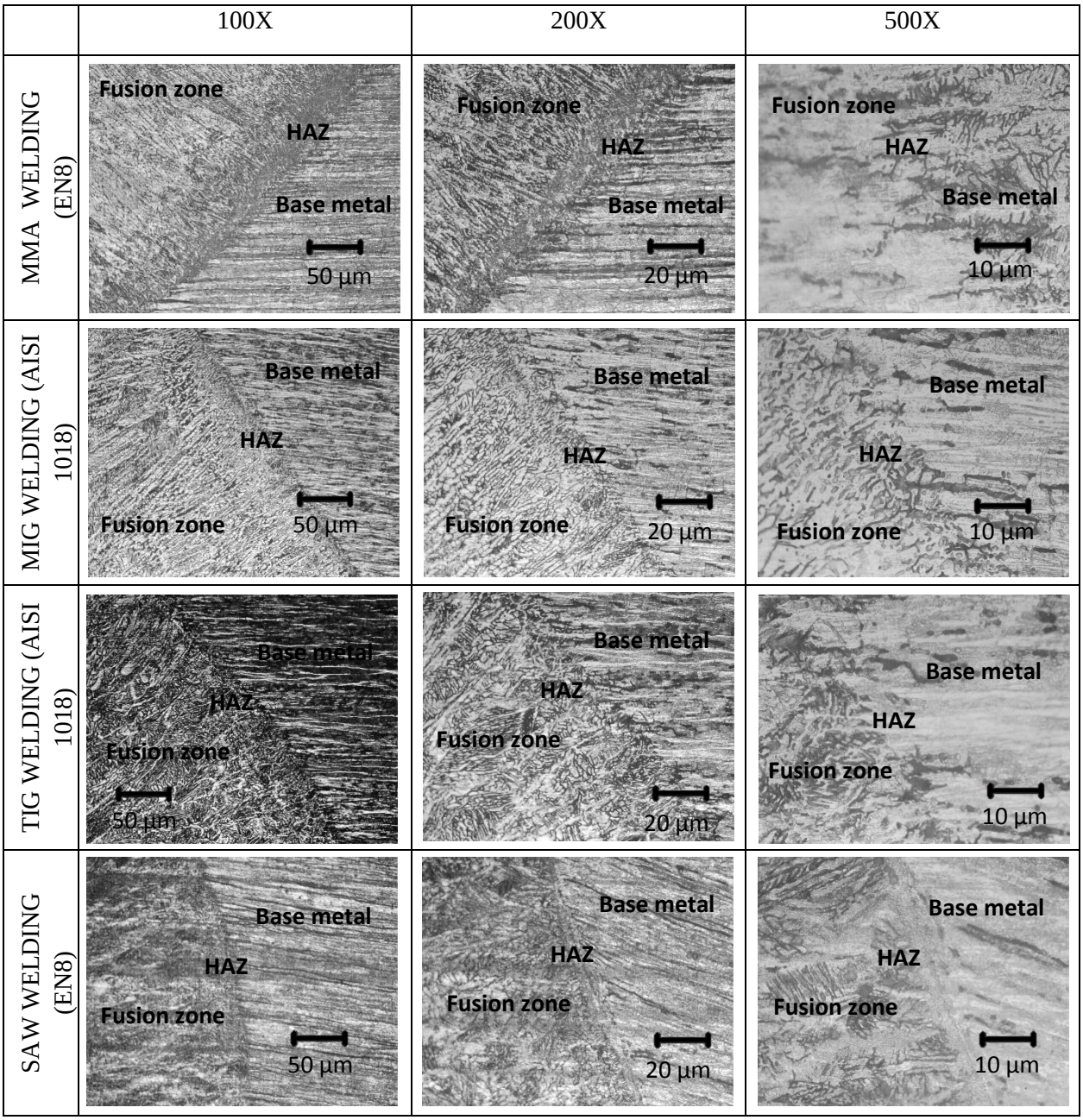

Figure 4.9: Microstructure analysis of as welded joints

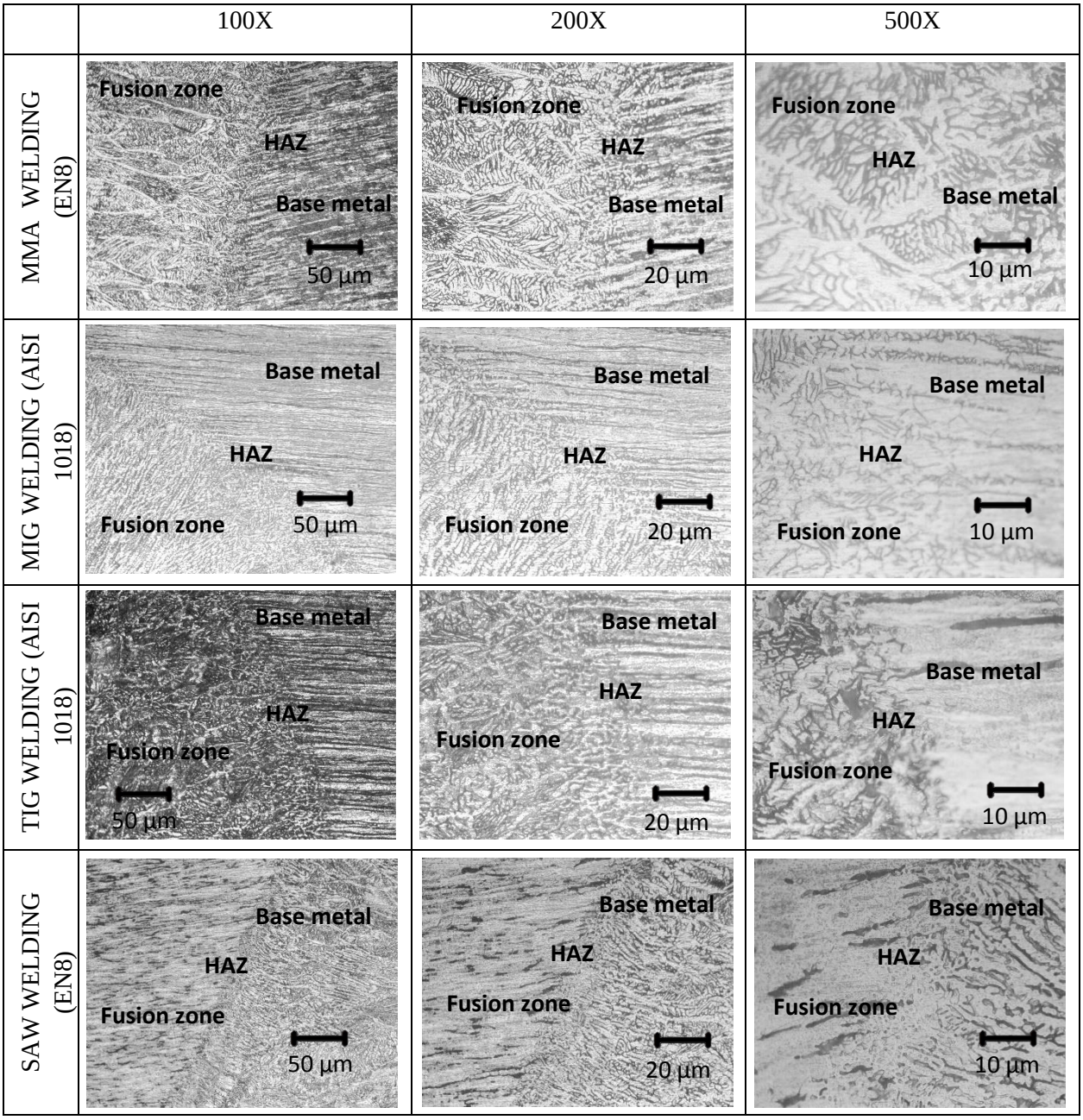

Figure 4.10: Microstructure analysis of abrasive blasted welded joints

The microstructure was observed at 100X, 200X and 500X. In fusion welding, dendrites grows from each grain point in one direction but this direction changes from grain to grain. Epitaxial growth dominates grain structure near the fusion line of weld when weld metal and base metal have same crystal structure. Direction prependicular to pool boundary is direction in which grains tends to grow during solidification because this has maximum temperature gradient so maximum heat extraction is in this direction. However in case of carbon steel (body centered cubic), columnar dendrites or cells within each grains tends to grow in easy growth direction (Chalmers, 1964). In fig 4.9 the FZ appears to contain a larger grain size than the HAZ, while a similar grain size order was found in MMA, MIG, TIG and SAW-welded joints. In the MMA, fusion zone having columnar dendrite structure was observed as an elongated grain structure due to a severe cooling rate. MIG has cellular grain structure while TIG and SAW has equiaxed dendritic structure. Apparently, the crystalline fusion zone structure is composed of a series of long grains, with dendrite directions that are spatially varied. It was found that the long columnar dendrite structure appeared to be nearly equiaxed. The base metal shows the same microstructure of both materials for their welded joints show same microstructure as there is no effect of welding on base metal. After the abrasive blasting treatment in fig. 4.10, it was found that grain structure gets reformed. The grain gets coarser which helps in improving the properties of weld joints. Coarser grains help in increasing microhardness of the weld joints. Finer the dendritic arm spacing, higher the ductility (Fukui and Namba, 1973) and yield strength of weld metal (Lanzafame and kattamis, 1973; Fukui and Namba, 1973).

4.4 Results of Tensile Test

Tensile test was carried out on as welded joints of both low carbon and medium carbon steel. Then Abrasive Blasting treatment was done at various time periods and again tensile strength was tested. Tensile specimen was prepared according to ASTM E-8 standards. The tensile test was carried out in Sri Guru Granth Sahib World University, Fatehgarh sahib. Figure 4.11 and 4.12 shows tensile specimens of low carbon steel and medium carbon steel.

Figure 4.11: Tensile test specimens of low carbon steel

Figure 4.12: Tensile test specimens of medium carbon steel

4.4.1 Results of Tensile Test on Low Carbon Steel:

MMA Welding:

Table 4.9 shows tensile strength values of MMA welding and fig. 4.13 shows bar graph of tensile strengths.

Table 4.9: Results of tensile strength of MMA welding on low carbon steel

Serial No.	Time Period (in min.)	Tensile Strength (N/mm^2)
1	0	359.0667
2	10	395.4667
3	15	419.8667
4	20	417.6
5	25	415.3333

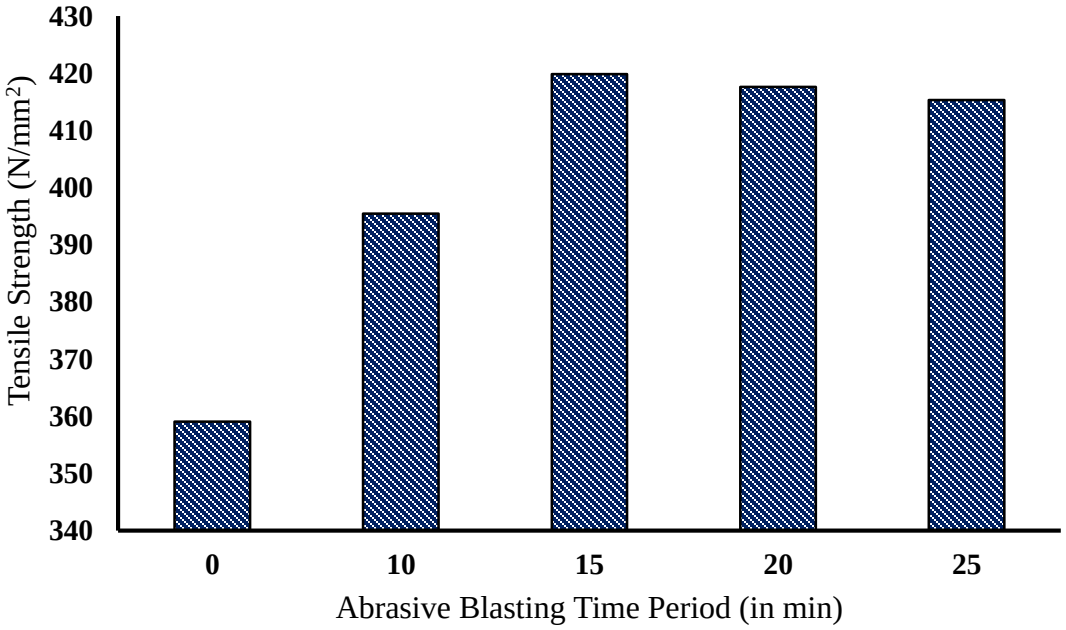

Figure 4.13: Tensile strength of MMA on low carbon steel

MIG Welding:

Table 4.10 shows tensile strength values of MIG welding and fig. 4.14 shows bar graph of tensile strengths.

Table 4.10: Results of tensile strength of MIG welding on low carbon steel

Serial No.	Time Period (in min.)	Tensile Strength (N/mm^2)
1	0	368.1333
2	10	413.4667
3	15	438.8
4	20	433.8667
5	25	429.4667

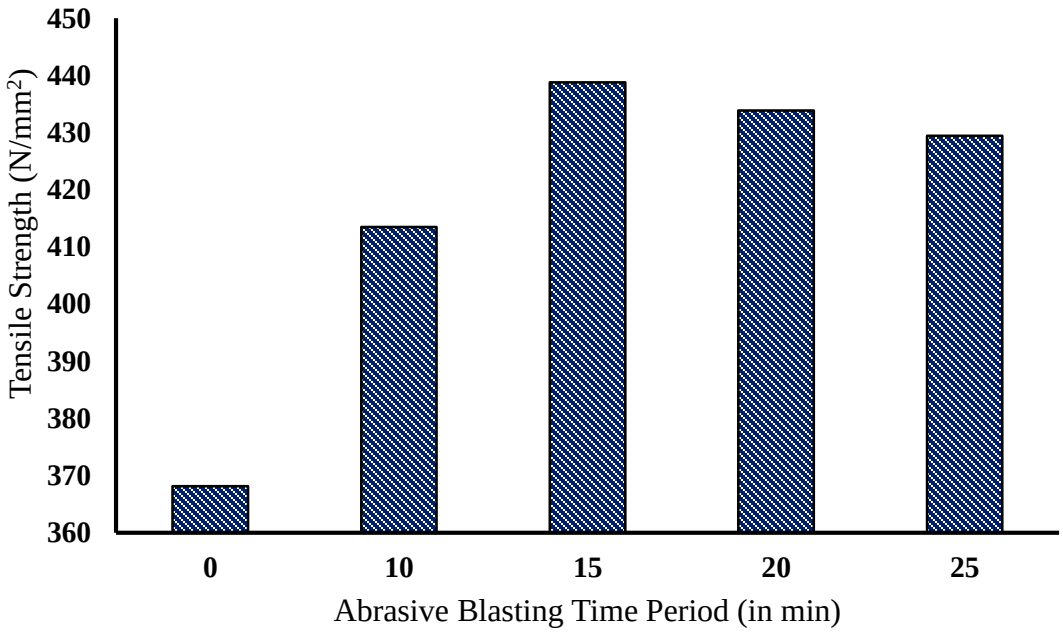

Figure 4.14: Tensile strength of MIG on low carbon steel

TIG Welding:

Table 4.11 shows tensile strength values of TIG welding and fig. 4.15 shows bar graph of tensile strengths.

Table 4.11: Results of tensile strength of TIG welding on low carbon steel

Serial No.	Time Period (in min.)	Tensile Strength (N/mm^2)
1	0	374.8
2	10	422.6667
3	15	446.1333
4	20	441.8667
5	25	437.0667

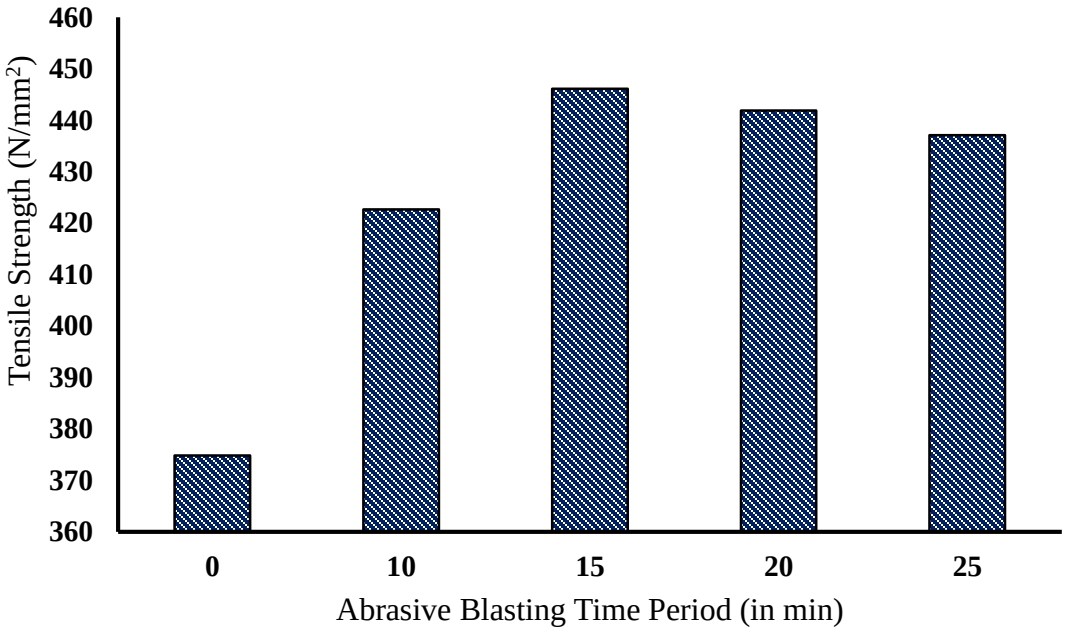

Figure 4.15: Tensile strength of TIG on low carbon steel

SAW Welding:

Table 4.12 shows tensile strength values of SAW welding and fig. 4.16 shows bar graph of tensile strengths.

Table 4.12: Results of tensile strength of SAW welding on low carbon steel

Serial No.	Time Period (in min.)	Tensile Strength (N/mm^2)
1	0	448.8
2	10	482.3333
3	15	499.9333
4	20	497.7333
5	25	495.0667

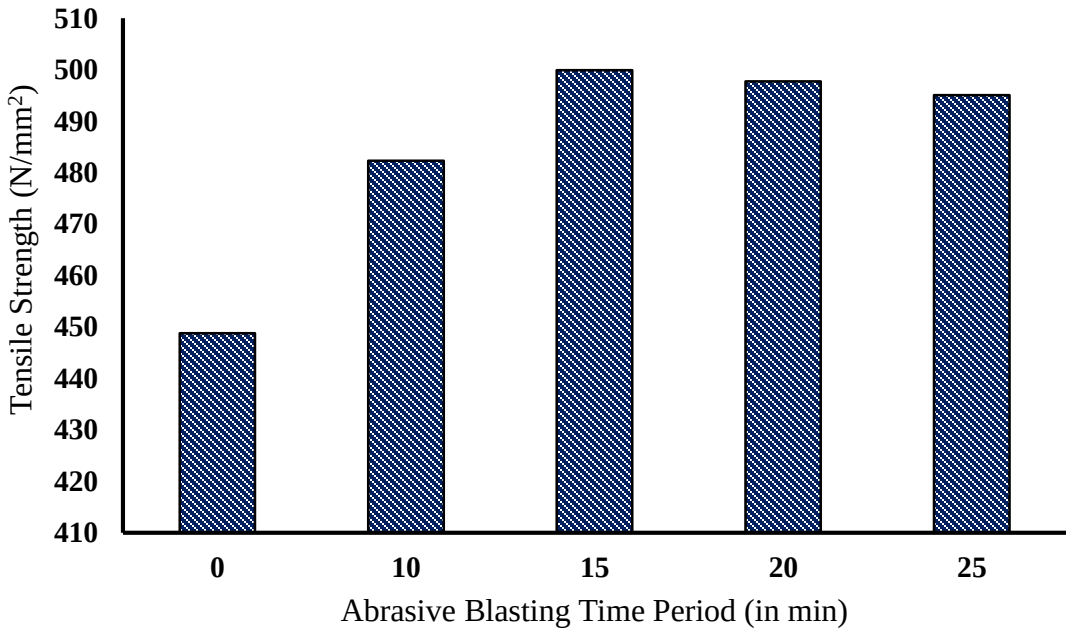

Figure 4.16: Tensile strength of SAW on low carbon steel

4.4.2 Results of Tensile Test on Medium Carbon Steel:

MMA Welding:

Table 4.13 shows tensile strength values of MMA welding and fig. 4.17 shows bar graph of tensile strengths.

Table 4.13: Results of tensile strength of MMA welding on medium carbon steel

Serial No.	Time Period (in min.)	Tensile Strength (N/mm^2)
1	0	437.4667
2	10	462.4
3	15	483.4667
4	20	477.8667
5	25	474.5333

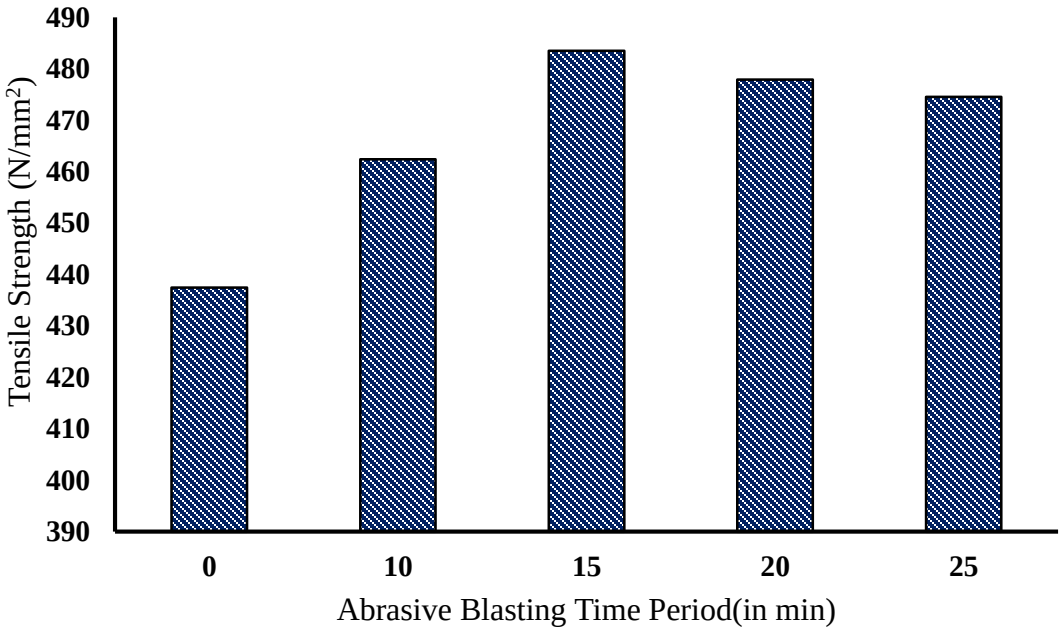

Figure 4.17: Tensile strength of MMA on medium carbon steel

MIG Welding:

Table 4.14 shows tensile strength values of MIG welding and fig. 4.18 shows bar graph of tensile strengths.

Table 4.14: Results of tensile strength of MIG welding on medium carbon steel

Serial No.	Time Period (in min.)	Tensile Strength (N/mm^2)
1	0	444.1333
2	10	469.0667
3	15	490
4	20	483.3333
5	25	478.2667

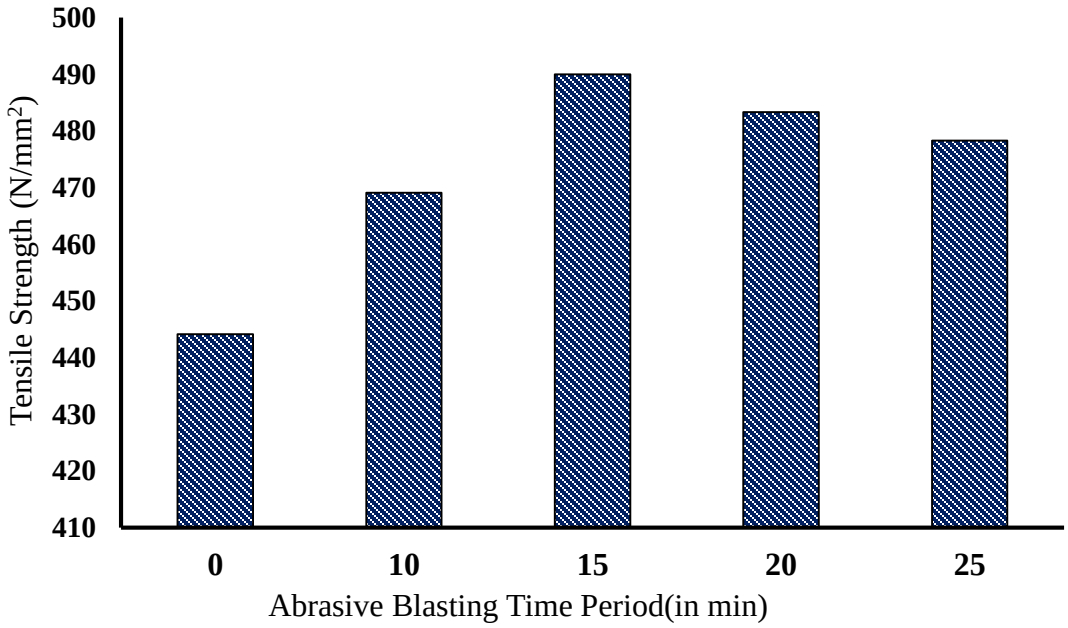

Figure 4.18: Tensile strength of MIG on medium carbon steel

TIG Welding:

Table 4.15 shows tensile strength values of TIG welding and fig. 4.19 shows bar graph of tensile strengths.

Table 4.15: Results of tensile strength of TIG welding on medium carbon steel

Serial No.	Time Period (in min.)	Tensile Strength (N/mm^2)
1	0	452.1333
2	10	478.2667
3	15	497.8667
4	20	490.8
5	25	487.8667

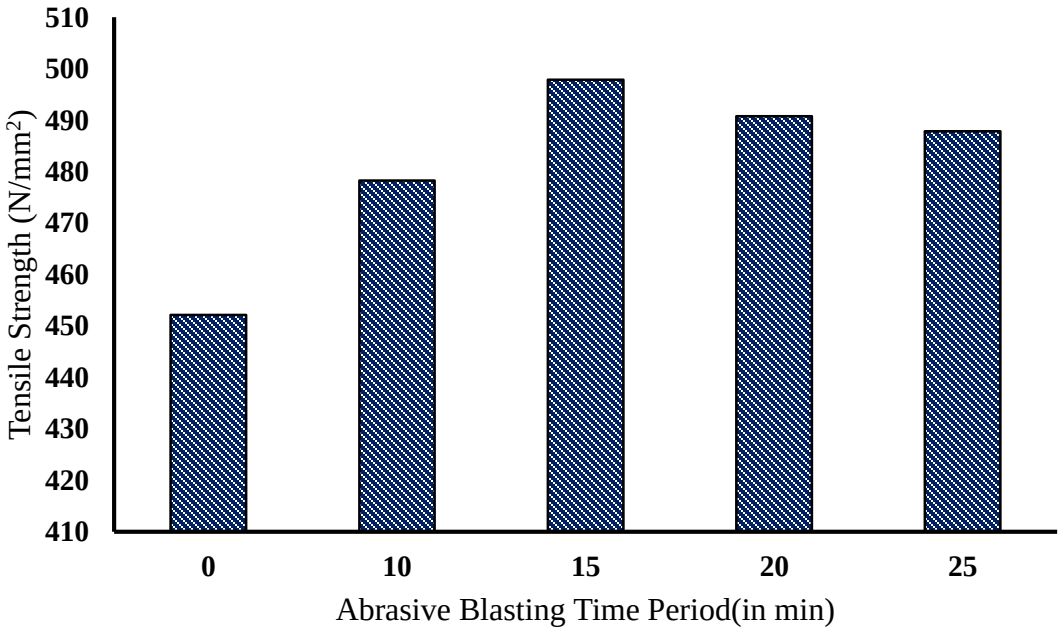

Figure 4.19: Tensile strength of TIG on medium carbon steel

SAW Welding:

Table 4.20 shows tensile strength values of SAW welding and fig. 4.20 shows bar graph of tensile strengths.

Table 4.16: Results of tensile strength of SAW welding on medium carbon steel

Serial No.	Time Period (in min.)	Tensile Strength (N/mm^2)
1	0	554.4667
2	10	584.9333
3	15	599.4667
4	20	590.1333
5	25	583.2667

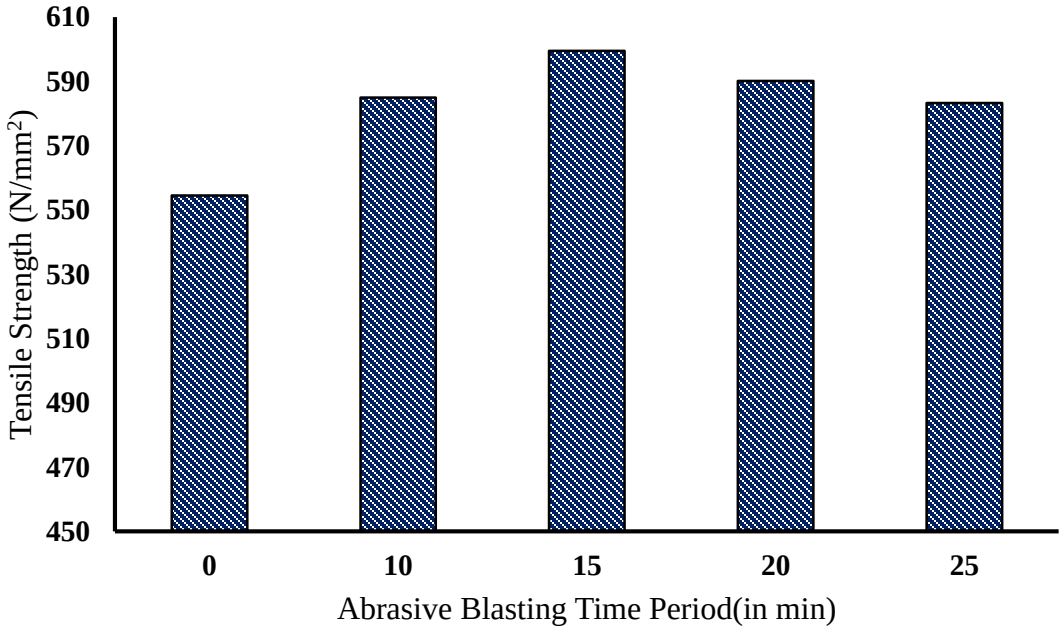

Figure 4.20: Tensile strength of SAW on medium carbon steel

Tables 4.9 to 4.16 shows the tensile strength of low carbon steel and medium carbon steel at MMA, MIG, TIG and SAW respectively. Fig. 4.13 to 4.20 shows the bar graph based upon the tensile strength for different fusion welded joints. Tensile strength specimen after breaking shows that almost all the workpieces broke from welded area. Tensile strength of welded joints increases due to abrasive blasting treatment. Tensile strength of MMA welding of low carbon steel of as welded joint is 359.0667 N/mm^2 which increases to 395.4667 N/mm^2 and 419.8667 N/mm^2 after 10 minutes and 15 minutes of abrasive blasting treatment respectively. After 15 minutes, if we increase the time period of blasting treatment, it slightly decreases the tensile strength. Tensile strength after 20 minutes and 25 minutes is 417.6 N/mm^2 and 415.3333 N/mm^2 respectively. Tensile strength of MIG welding of as welded and at different time periods in N/mm^2 are 368.1333, 413.4667, 438.8, 433.8667 and 429.4667. Tensile strength of TIG welding of as welded and at different time periods in N/mm^2 are 374.8, 426.667, 446.133, 441.867 and 437.0667. Tensile strength of SAW welding of as welded and at different time periods in N/mm^2 are 448.8, 482.3333, 499.9333, 497.7333 and 495.0667. For medium carbon steel tensile strength shows the same trend of tensile strength increment till 15 minutes then slight decrement in tensile strength values. The reason in increment of tensile strength is due to induced residual compressive stresses. The abrasive blasting balls acts like tiny hammers and causes permanent plastic deformation which induces the compressive stresses which annuls out the effect of tensile stresses produced during welding. The reduction in tensile strength after 15 minutes can be due to increased brittleness or due to some other reason.

4.5 Fractographic Analysis

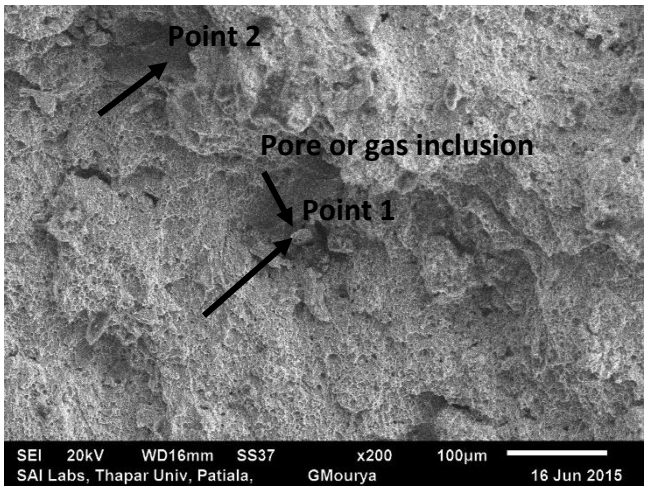

(a)

Element Wt%	1	2
C	7.17	4.99
O	5.07	12.22
Si	0.58	0.48
Mn	0.38	0.45
Fe	86.8	81.86

(b)

Figure 4.21: (a) SEM fractography image of MMA welded joint of low carbon steel (b) EDS spectrum and its elements

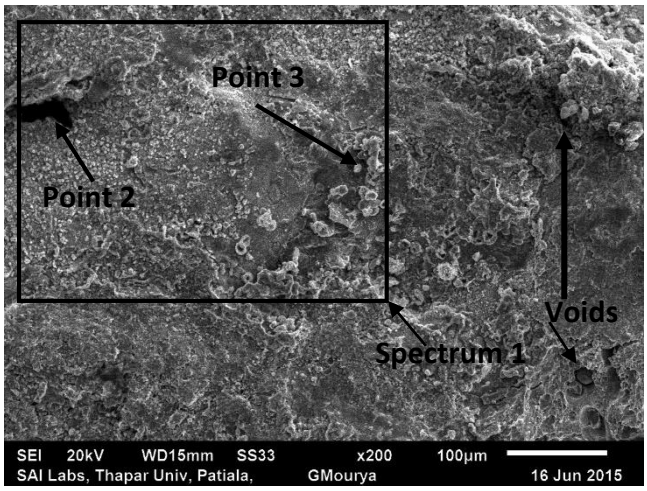

(a)

Element Wt%	1	2	3
C	10.14	6.66	11.72
O	35.56	32.31	21.54
Si	2.16	0.48	0.51
Mn		0.45	0.3
Fe	52.14	60.10	65.93

(b)

Figure 4.22: (a) SEM fractography image of TIG welded joint of low carbon steel (b) EDS spectrum and its elements

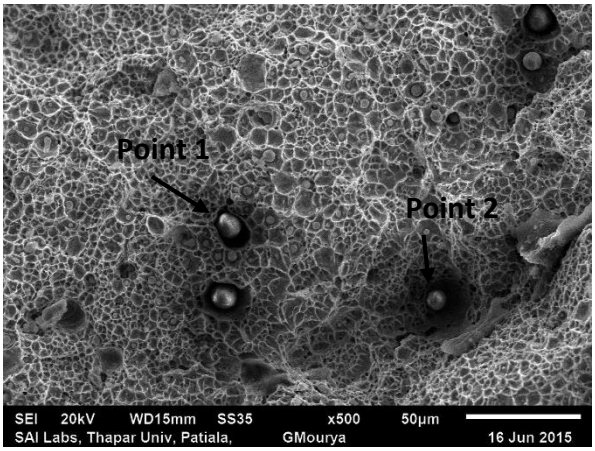

(a)

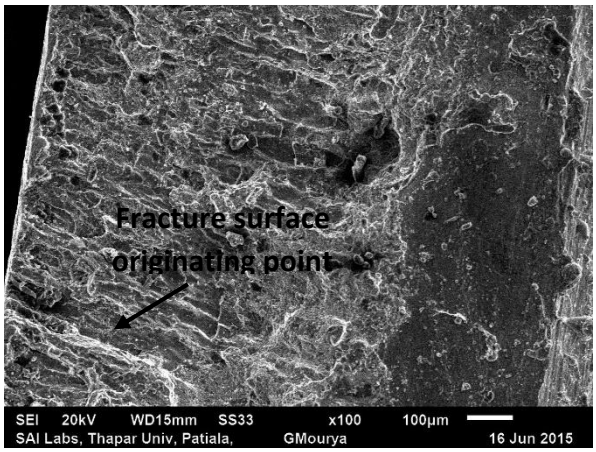

(b)

Element Wt%	1	2
C	6.88	6.78
O	35.99	12.71
Si	16.46	1.35
Mn	15.56	1.96
Fe	22.61	84.86
Al	0.88	
S	0.47	
Ti	1.14	

(c)

Figure 4.23: (a) SEM fractography image of MIG welded joint of medium carbon steel (b) fractured surface area enlarged (c) EDS spectrum and its elements

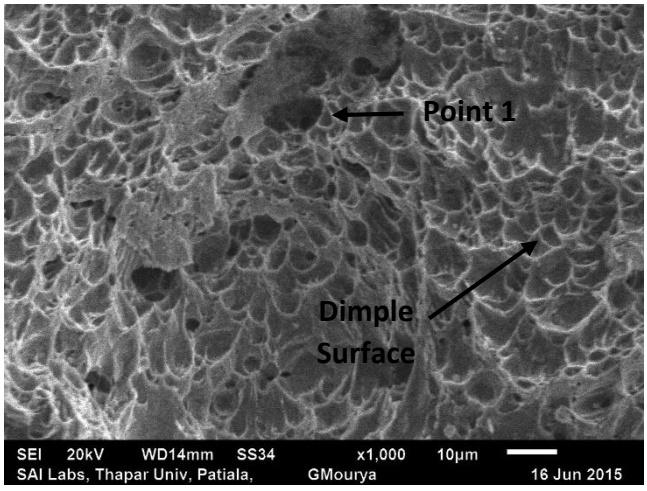

(a)

Element Wt%	1
C	4.92
O	26.93
Si	2.46
Mn	5.57
Fe	58.4
Al	0.6
Cr	1.11

(b)

Figure 4.24: (a) SEM fractography image of TIG blasted welded joint of medium carbon steel (b) EDS spectrum and its elements

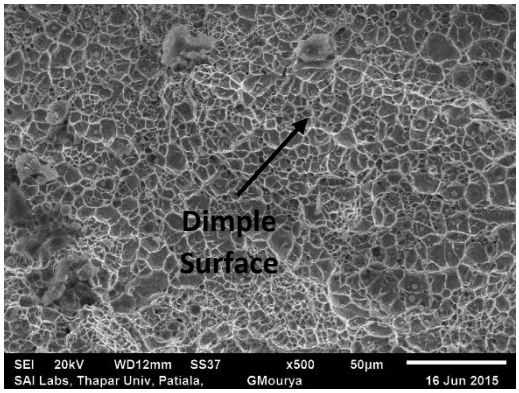

(a)

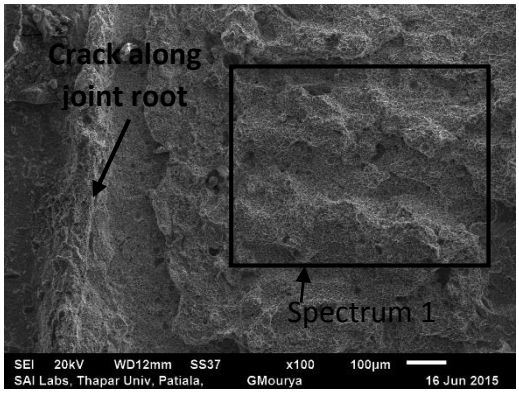

(b)

Element Wt%	1
C	7.95
O	5.46
Si	0.99
Fe	84.34
Na	1.26

(c)

Figure 4.25: (a) SEM fractography image of MMA blasted welded joint of medium carbon steel (b) fractured surface area enlarged (c) EDS spectrum and its elements

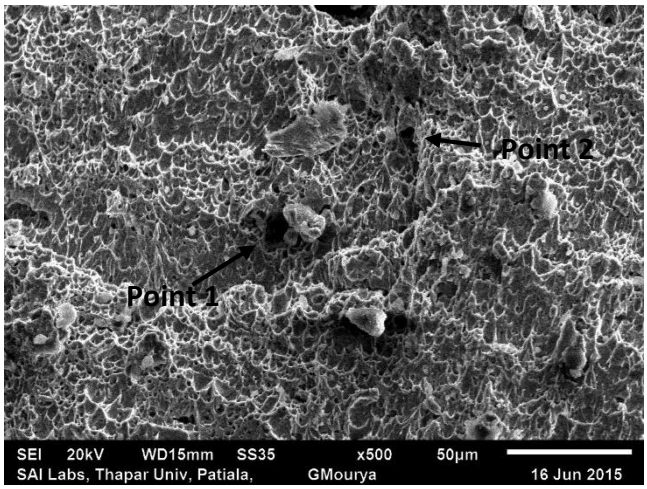

Element Wt%	1	2
C	60.31	16.92
O	33.92	7.81
Si		0.82
Mg	0.36	
Fe	1.68	74.45
Ca	2.92	
S	0.82	

(a) (b)

Figure 4.26: (a) SEM fractography image of MIG welded joint of low carbon steel (b) EDS spectrum and its elements

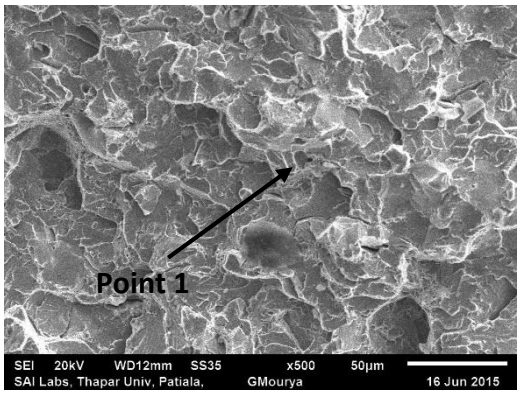

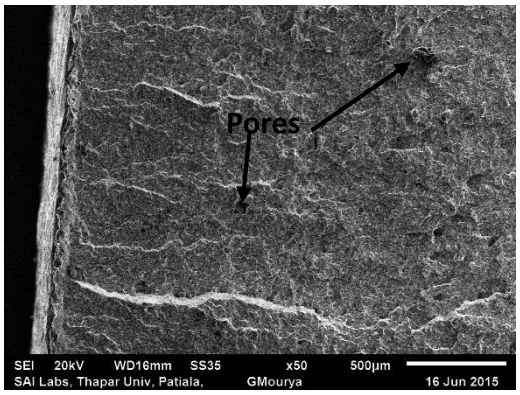

(a) (b)

Element Wt%	1
C	13.42
O	8.59
Si	0.48
Fe	77.13
Mn	0.38

(c)

Figure 4.27: (a) SEM fractography image of SAW welded joint of medium carbon steel (b) fractured surface area enlarged (c) EDS spectrum and its elements

Fig. 4.21 to 4.27 reveals that three main elements were found in the MMA, MIG, TIG and SAW welded joints, which were identified as carbon, iron, and oxygen. It can be seen that the distribution of the carbon content is non-uniform depending on the type of welding applied. Overall, the inclusions observed in the MMA-welded joint were SiO2 inclusions as well as a small amount of Na element. The analysis shows that a mixture of Al2O3–SiO2 inclusions were found in the MIG-welded joint and only MnO was found in the TIG-welded joint. Additionally, the Fe content is believed to originate from the steel matrix. The above presence of inclusions (mainly oxides) is known to influence fracture behavior, and the scatter of oxides (which may cause degradation in fatigue performance) in the fusion zones may be attributed to the manually handled welding process. The SEM indicate that: (1) the MMA-welded joint shows lack of penetration (LOP) due to failure to achieve complete penetration at the root of the weld and (2) there is a cap undercut at the weld bead. A similar LOP was found in the MMA blasted joint. On the other hand, the discontinuities defined in the MIG welded joint appears as a dark grey round or irregular spot and occur in a row. This type of discontinuity is defined as porosity and is produced due to entrapment of gas in the weld during the welding procedure. Furthermore, the TIG-welded and peened skimmed joints displayed dark round irregular spots in the middle of the weldment It is evident that LOP is considered as a defect and may cause dangerous failure, in contrast to porosity or gas holes.

Overall, all as-welded and blasted samples failed or fractured in a direction normal to the maximum tensile stress direction. Microscopically, fractures initiate at surface irregularities or most likely at internal inhomogeneities such as voids or inclusions. The MMA-welded joint shows evidence of beachmark due to tensile failure. Further magnification with SEM analysis confirmed the existence of trapped gaseous elements within the weld regime. The dimple fracture surface is shown in TIG-welded joint; its fibrous and rough surface showed that the crack propagated inside, causing severe damage to the weld joint. It is mainly composed of iron (about 93.36%), showing the hardest FZ region due to the tensile loading. At this point, there was no evidence or clear indication of an oxide inclusion or gas entrapment. The presence of a well-defined river pattern or beachmark is observed as initiated at the surface of the specimen, which was formed predominantly from the free surface roughness of the MMA-peened skimmed joint. It was observed that the surface of the MMA-peened welded joint is tortuous and grey. The analysis confirmed the existence of voids or dimples and a rough appearance, which is believed to be due to LOP during the welding practice.

Based on Fig. 4.26b, the EDX analysis confirms the existence of 60.31 % oxygen in the MIG-welded joint. Tracing the discontinuity evidence, the crack was originated in a pore where a high level of oxygen element was found. Fig. 4.24a shows the fracture surface of a TIG welded joint which confirms the evidence of porosity in the middle of the weld bead surface. The porosity was found to be located in the subsurface of WM region. It is believed that discontinuities such as porosity located in the WM are of special concern, since high tensile residual stresses develop from the welding process.

Chapter 5

Conclusions and Scope for Future Work

5.1 Conclusions

The effect of abrasive blasting treatment on fusion welded joints of low carbon and medium carbon steel are studied. Various tests were done to find out the mechanical properties of the weld.

- Microhardness test on both low carbon and medium carbon steel shows that abrasive blasting treatment increases the VHN values at all zones. There is a significant amount of increment till 15 minutes but later on there is less increment in microhardness values. VHN values increases due to permanent plastic deformation induced in the surface thus producing beneficial stresses in the material. Abrasive blasting also improves the grain structure which also helps in increase of hardness. The average value of fusion zone of low carbon steel of MMA joint increases from 191.3486 to 256.6593, of MIG joint increases from 185.6992 to 249.0028, of TIG joint increases from 192.2104 to 261.1422 and of SAW increases from 200.1738 to 269.8598. The values show that SAW gives highest hardness values but it can be only used for plates thicker than 10 mm. For thin plates, TIG welding gives best result. In case of medium carbon steel the average value of VHN of MMA increases from 215.414 to 251.1009, of MIG increases from 218.4417 to 272.1739, of TIG increases from 217.0460 to 280.5931 and of SAW increases from 220.3155 to 288.4897. The VHN values of medium carbon steel also shows that TIG welding gives best result for smaller thickness plates otherwise SAW gives best result.
- Tensile test on both low carbon steel and medium carbon steel shows that tensile strength increases due to abrasive blasting treatment. Tensile strength increases till 15 minutes, after that there is slight decrease in value. Abrasive blasting treatment increases ductility of the material thus increasing tensile strength. Abrasive blasting also induces residual compressive stress which counters the tensile stress produced during welding helping in increment of tensile strength. Maximum tensile strength observed for low carbon steel for MMA, MIG, TIG and SAW joints are 419.8667, 438.8, 446.133 and 499.9333 respectively. Thus we can conclude that SAW gives a better weld joint. For thin plates TIG is the best

available option. In case of medium carbon steel maximum tensile strength observed for MMA, MIG, TIG and SAW joints are 483.4667, 490, 497.8667 and 599.4667 respectively. SAW is the best option for welding thicker plates. For thin plates TIG is the best option.

- Microstructure study reveals that abrasive blasting treatment improves the grain size. The grain becomes coarser, thus increasing the microhardness and tensile strength of the material. MMA has cellular dendritic structure, TIG has columnar dendritic structure, MIG and SAW has equiaxed dendritic structure.
- Fractography reveals that fracture starts from irregularities in the surface. The irregularities found in the surface are voids, lack of penetration, pores, gas inclusions and undercuts. The major elements found in EDS of the weld joints are Fe, C and O. There are also traces of Na, Cl, Si and Mn. Oxygen combines with elements and form oxides reducing the properties of the material.

5.2 Scope for Future Work

- Various welding parameters like current, voltage, welding speed etc. can be considered for optimization while optimizing abrasive blasting treatment.
- By using the same factors and data, other optimization techniques like RSM method, fuzzy logic can be applied and different results can be compared.
- Different post welding treatment can be applied and its results can be compared to abrasive blasting treatment.
- Effect of different abrasive blasting media on welded joints can be observed.
- Effect of time period of abrasive blasting treatment on welded joints can be optimized using various optimization techniques.

REFERENCES

Abdullah, A.; Malaki, M.; Eskandari, A. (2012) Strength enhancement of the welded structures by ultrasonic peening. *Materials and Design*, 38; 7–18.

Akinlabi, E.T.; Ogunmuyiwa, E.; Akinlabi, S. A. (2013) Characterizing the effects of sand blasting on formed steel samples. *International Journal of Mechanical, Aerospace, Industrial and Mechatronics Engineering*, Vol: 7, No: 11.

Ali, A.; An, X.; Rodopoulos, C.A.; Brown, M.W.; Hara, P. O; Levers, A.; Gardiner, S. (2007) The effect of controlled shot peening on the fatigue behavior of 2024-T3 aluminum friction stir welds. *International Journal of Fatigue*, 29; 1531–1545.

Aparicio, C.; Gil, F.J.; Fonseca, C., Barbosa; M., Planell; J.A. (2003) Corrosion behavior of commercially pure titanium shot blasted with different materials and sizes of shot particles for dental implant applications. *Biomaterials*, 24; 263–273.

Berezhnyts'ka, M.P.; Huslyakova, H.P.; Tkachov, V.I. (2000) Enhancement of the durability of structural steels and their welded joints by plastic deformation. *Materials Science*; Vol. 36. No. 3; 463-465.

Byrne, G.D.; O'Neill, L.; Twomey, B.; Dowling, D.P. (2013) Comparison between shot peening and abrasive blasting processes as deposition methods for hydroxyapatite coatings onto a titanium alloy. *Surface and Coatings Technology*, 216; 224–231.

Chalmers B. (2001) Principles of Solidification. *Wiley, New York,* 1964.

Fukui, T.; Namba, K. (1973) Solidification of fusion welding. *Trans. Japan Weld Society*; 4:49.

Ghosh, A.; Mallik, A.K. (2010) Manufacturing Science. *Affiliated East–West Press*, 1985.

Habibi, N.; H- Gangaraj, S.M.; Farrahi, G.; Majzoobi, G.H.; Mahmoudi, A.H.; Daghigh, M.; Yari, A.; Moridi, A. (2012) The effect of shot peening on fatigue life of welded tubular joint in offshore structure. *Materials and Design, 36*; 250–257.

Hasegawa, M.; Suzuki, H.; Miura, K. (2009) Effect of strong shot peening cleaning and hot galvanizing on fatigue strength of steel welded joint. *Welding International*, 23:5; 360-368.

Hasegawa, H.; Ohta, K.; Suzuki, H. (2004) Improvement of fatigue strength of SM490A welded joints by high-hardness/high-specific gravity shot peening. *Welding International*, 18:3; 181-188.

Hatamleh, O.; Lyons, J.; Forman, R. (2007) Laser and shot peening effects on fatigue crack growth in friction stir welded 7075-T7351 aluminum alloy joints. *International Journal of Fatigue*, 29; 421–434.

Hatamleh, O. (2009a) A comprehensive investigation on the effects of laser and shot peening on fatigue crack growth in friction stir welded AA 2195 joints. *International Journal of Fatigue*, 31; 974–988.

Hatamleh, Omar; DeWald, Adrian (2009b) An investigation of the peening effects on the residual stresses in friction stir welded 2195 and 7075 aluminum alloy joints. *Journal of Materials Processing Technology*, 209; 4822–4829.

Hatamleh, O.; Mishra, R.S.; Oliveras, O. (2009c) Peening effects on mechanical properties in friction stir welded AA 2195 at elevated and cryogenic temperatures. *Materials and Design*, 30; 3165–3173.

Hatamleh, O.; Smith, J.; Cohen, D.; Bradley, R. (2009d) Surface roughness and friction coefficient in peened friction stir welded 2195 aluminum alloy. *Applied Surface Science*, 255; 7414–7426.

Hui, Z.Z.; Kai, G.S.; Fei, L.H.; Bin, X.H.; Gang, Z.C.; Lu, W. (2007) Effects of Shot Peening Process on Thermal Cycling Lifetime of TBCs Prepared by EB-PVD. *Chinese Journal of Aeronautics*, 20; 145-147.

Kameyama, Y.; Komotori, J. (2009) Effect of micro ploughing during fine particle peening process on the microstructure of metallic materials. *Journal of Materials Processing Technology*, 209; 6146–6155.

Kennedy, D.M.; Vahey, J.; Hanney, D. (2005) Micro shot blasting of machine tools for improving surface finish and reducing cutting forces in manufacturing. *Materials and Design*, 26; 203–208.

Kim, In-Tae (2013) Fatigue strength improvement of longitudinal fillet welded out-of-plane gusset joints using air blast cleaning treatment. *International Journal of Fatigue*, 48; 289–299.

Lah, N.A.C.; Ali, A.; Ismail, N.; Chai, L. P.; Mohamed, A.A. (2010) The effect of controlled shot peening on fusion welded joints. *Materials and Design*, 31; 312–324.

Lanjafame, J.N.; Kattamis, T.Z. (1973) Effect of grain size on yield strength. *Welding Journal*; 52, 226

Lobanov, L.M.; Kyr'yan, V.I.; Knysh, V.V. (2006) Enhancement of the service life of welded metal structures by high-frequency mechanical peening. *Materials Science*, Vol. 42, No. 1; 54-60.

Meo, M.; Vignjevic, R. (2003) Finite element analysis of residual stress induced by shot peening process. *Advances in Engineering Software*, 34; 569–575.

Naidu, N.K.R.; Raman, S.G.S. (2005) Effect of shot blasting on plain fatigue and fretting fatigue behavior of Al–Mg–Si alloy AA6061. *International Journal of Fatigue*, 27; 323–331.

Salman, H.S.; Khethier, A.M.; Mohammed, A.A.H. (2015) Effect of shot peening on the mechanical properties for welded joints of Aluminum Alloy 6061-T6. *Full Paper Proceeding NDMRP-2015,* Vol. 2; 43-56.

Sano, Y.; Masaki, K.; Gushi, T.; Sano, T. (2012) Improvement in fatigue performance of friction stir welded A6061-T6 aluminum alloy by laser peening without coating. *Materials and Design*, 36; 809–814.

Sidhom, N.; Laamouri, A.; Fathallah, R.; Braham, C.; Lieurade, H.P. (2005) Fatigue strength improvement of 5083 H11 Al-alloy T-welded joints by shot peening: experimental characterization and predictive approach. *International Journal of Fatigue*, 27; 729–745.

Śledź, M.; Bąk, Ł.; Stachowicz, F.; Zielecki, W. (2013) Analysis of the effect of shot peening on mechanical properties of steel sheets used as screener sieve materials. *Journal of Physics: Conference Series*, 451; 012029.

Tsujikawa, M.; Egawa, M.; Sone, T.; Ueda, N.; Okano, T.; Higashi, K. (2013) Modification of S phase on austenitic stainless steel using fine particle shot peening. *Surface and Coatings Technology*, 228; S318–S322.

Zhao, X.; Wang, D.; Huo, L. (2011) Analysis of the S–N curves of welded joints enhanced by ultrasonic peening treatment. *Materials and Design*, 32; 88–96.

Zivkovic, D.; Anzulovi, B. (2005) The fatigue of 5083 aluminum alloy welds with the shot-peened crater hot-cracks. *Materials and Design*, 26; 247–250.